



Groundwater - Mediated Influences of Beaver - Mimicry Stream Restoration: A Modeling Analysis

Andrew L. Bobst, Robert A. Payn, Glenn D. Shaw

This is the peer reviewed version of the following article: [Groundwater - Mediated Influences of Beaver - Mimicry Stream Restoration: A Modeling Analysis. JAWRA Journal of the American Water Resources Association (2022)], which has been published in final form at <https://doi.org/10.1111/1752-1688.13044>. This article may be used for non-commercial purposes in accordance with Wiley Terms and Conditions for Use of Self-Archived Versions: <https://authorservices.wiley.com/author-resources/Journal-Authors/licensing/self-archiving.html#3>.

1 **Groundwater-Mediated Influences of Beaver-Mimicry Stream Restoration: A**
2 **Modeling Analysis**

3 *Andrew L. Bobst, Robert A. Payn, and Glenn D. Shaw*

4 Department of Land Resource & Environmental Sciences (Bobst, Payn), Montana State
5 University, Bozeman Montana, USA; Department of Geological Engineering (Shaw), Montana
6 Technological University, Butte Montana, USA (Correspondence to Bobst: abobst@mtech.edu).

7

8 **Research Impact Statement:** Some purported benefits of beaver-mimicry stream restoration
9 require changes in groundwater flow. Models allow exploration of patterns in groundwater-
10 mediated effects of different design strategies.

11

12 **ABSTRACT:** Beaver-mimicry stream restoration (BMR) involves alteration of a stream channel
13 to approximate the effects of beaver activity. Project objectives often include increasing
14 groundwater storage and dry-season streamflow, but limited data are available to understand the
15 nature of its effects on groundwater dynamics. We developed generic groundwater models of
16 mountain headwater streams to investigate the effects of installing a single beaver mimicry
17 structure (BMS) using different restoration designs in varied hydrogeologic settings. The
18 magnitude of changes in dry-season net stream gains from a single BMS were always a minor
19 component of the channel water balance, and would be too small to measure in the field;
20 however, the modeled patterns of change caused by a single BMS help to understand the
21 underlying mechanisms. All tested scenarios caused increases in groundwater recharge from the
22 stream, which resulted in increased groundwater levels, and groundwater outflow from the model
23 domain. For scenarios that did not include evapotranspiration, most treatments in gaining and
24 losing settings caused slight increases in dry-season net stream gains, but in strongly losing
25 settings net stream gains were reduced. The addition of simulated evapotranspiration often
26 resulted in decreased dry-season net stream gains, since evapotranspiration increased with
27 groundwater elevations. BMR design and siting influence the types of hydrologic effects that
28 should be anticipated.

29 **(KEYWORDS:** hydrology, streamflow, ground water hydrology, surface water/ground water
30 interactions, drought)

INTRODUCTION

31
32 Evident shifts in the climate at higher elevations suggest that consideration of changes in
33 seasonal to interannual water storage should be a high priority for water planning in mountainous
34 watersheds. Field observations and climate change predictions from extensive literature
35 regarding mountainous areas indicate that snowpack accumulation is likely to decline and that
36 accumulated snow is likely to melt earlier in the year, which will result in lower dry-season
37 streamflows (Barnett *et al.*, 2005; Cayan *et al.*, 2001; Clow, 2010; Naz *et al.*, 2018). Shifts in
38 precipitation from snow to rain is a major driver of reduced snowpack (Berghuijs *et al.*, 2014;
39 Knowles *et al.*, 2006), which is expected to diminish seasonal hydrologic storage even where
40 total annual precipitation increases. Stream restoration projects that increase seasonal (or longer)
41 hydrologic storage can be used to mitigate this loss of snowpack storage in an attempt to sustain
42 fluvial corridor ecosystems and human infrastructure.

43 With a common objective to increase water storage, beaver-mimicry stream restoration
44 (BMR) is becoming an increasingly common practice (Bouwes *et al.*, 2016; Lautz *et al.*, 2019;
45 Pollock *et al.*, 2014, 2018; Weber *et al.*, 2017). These projects typically include the installation
46 of multiple in-stream beaver-mimicry structures (BMSs; a.k.a. beaver dam analogs) that are
47 designed to have an ecohydrological function similar to beaver dam complexes (Pollock *et al.*,
48 2018; Lautz *et al.*, 2019; Nash *et al.*, 2021; Pilliod *et al.*, 2018). BMSs include an on-channel
49 structure and an associated upstream pool, which causes the stage of the stream and adjacent
50 groundwater levels to increase upstream of the structure. The treatments may also include
51 activation of side channels at high flows, inundation of the floodplain during high flows, or
52 seasonal filling of off-channel ponds. The additional seasonal inundation caused by BMSs often
53 enhances groundwater recharge, and they are often advertised to increase dry-season
54 streamflows.

55 Numerous studies have provided observational evidence that natural beaver activity and
56 BMR increase groundwater levels in the alluvial aquifer, typically by less than 1 m (Bouwes *et*
57 *al.*, 2016; Janzen and Westbrook, 2011; Majerova *et al.*, 2015; Pollock *et al.*, 2018; Westbrook *et*
58 *al.*, 2006). Some investigations have observed little change in groundwater levels following the
59 implementation of BMR or wet meadow restoration projects (Klein *et al.*, 2007; Scamardo and
60 Wohl, 2020), suggesting that the observed changes in groundwater elevations are dependent on
61 the type of treatment used, the hydrogeologic setting, and the monitoring design. Dry-season
62 streamflows are often suggested to increase following BMR; however, quantifications of these
63 increases have been limited, likely due to the difficulty in quantifying small changes in
64 streamflow with confidence (Bouwes *et al.*, 2016; Burns and McDonnell, 1998; Gurnell, 1998;
65 Hunt *et al.*, 2018; Janzen and Westbrook, 2011; Majerova *et al.*, 2015; Nyssen *et al.*, 2011;
66 Pollock *et al.*, 2007, 2018; Wegener *et al.*, 2017; Westbrook *et al.*, 2006). Some researchers have
67 suggested that increases in streamflow due to wet-meadow restoration will be too small to
68 measure and the higher groundwater elevations would also cause higher groundwater
69 evapotranspiration (ET_{gw}) (Nash *et al.*, 2018, 2020). This increase in ET_{gw} may more than offset
70 the increased net stream gains that would be otherwise be expected. While the changes in
71 surface-water storage due to the creation of on-channel ponds behind BMSs are evident, the
72 changes in groundwater flow patterns relevant to driving seasonal subsurface storage are not well
73 understood, especially in the context of project designs that are most likely to meet hydrologic
74 objectives.

75 When groundwater recharge increases along a restored stream reach, the additional water
76 will ultimately be partitioned between different potential outputs from the reach, such as
77 groundwater discharge to the stream, down-valley groundwater outflow, or evapotranspiration.

78 Aquifer properties and the proximity of seasonal groundwater mounds to surface waters will
79 determine the time needed for higher hydraulic heads to propagate through the aquifer and
80 increase groundwater discharge to streams (Bredehoeft, 2002; Bredehoeft *et al.*, 1982; Kendy
81 and Bredehoeft, 2006; Theis, 1940). The concept of mounding helps to aggregate perspectives on
82 the timing of both water and energy movement through the alluvial aquifer.

83 Past research has demonstrated that streams with more sinuosity or more complex bed
84 topography (e.g. pool-riffle sequences, beaver dams, or BMSs) exhibit more hyporheic exchange
85 between the stream and the underlying aquifer under steady-state conditions (Cardenas, 2008,
86 2009; Cardenas *et al.*, 2004; Gomez-Velez *et al.*, 2017; Harvey and Bencala, 1993; Kasahara and
87 Hill, 2006; Kasahara and Wondzell, 2003). Work in the steady-state perspective has been critical
88 to understanding the fundamental drivers of stream-subsurface exchange, but the need for more
89 dynamic and scalable conceptualizations of hyporheic flow has become clear as the attention of
90 land managers is shifting toward seasonal water storage for ecosystem or human demands
91 (Gomez-Velez *et al.*, 2017). For example, modeling of transient hyporheic exchange or lateral
92 contributions from hillslopes has shown that variations in alluvial groundwater levels over time
93 play an important role in determining the exchange of water between streams and their
94 associated alluvial aquifers (Boutt and Fleming, 2009; Chen and Chen, 2003; Gomez-Velez *et*
95 *al.*, 2017; Malzone *et al.*, 2016; Schmadel *et al.*, 2016; Ward *et al.*, 2017; Woessner, 2000;
96 Wroblicky *et al.*, 1998). Short-term variations in stream stage due to diel cycles or storm events
97 have also been shown to cause substantial lateral water exchange between surface waters and the
98 banks, resulting in bank storage (Gomez-Velez *et al.*, 2017; Sawyer *et al.*, 2009). Studies of
99 changes in storage dynamics due to wet-meadow restoration on gaining streams suggest that
100 groundwater levels rise in response to the treatment, but these increases do not result in

101 meaningful changes in groundwater discharge to the stream during the dry season (Nash *et al.*,
102 2018). Dynamic models of hyporheic water exchange that include periodic off-channel
103 inundation have only rarely been developed to understand the influence of changing groundwater
104 recharge (Helton *et al.*, 2014), and to our knowledge have not been developed to understand the
105 related hydrologic effects of BMR activities. From this perspective, stream restorations that are
106 intended to increase seasonally dynamic hydrologic storage may be treated as manipulative
107 experiments with potential to advance the evolving science of fluvial corridor hydrology (Harvey
108 *et al.*, 2019).

109 The potential for stream restoration to influence seasonal water storage in local alluvial
110 aquifers partly depends on the hydrogeologic setting that determines the overall gaining or losing
111 nature of the stream (Larkin and Sharp, 1992; Winter *et al.*, 1998; Woessner, 2000). Stream
112 reaches where alluvial groundwater elevations are substantially lower than the streambed are
113 unlikely to experience local increases in dry-season net stream gains since the resulting
114 groundwater mounds would be unlikely to be of sufficient magnitude to reverse or reduce stream
115 loss during the dry season. In contrast, where groundwater levels are substantially higher than the
116 stream stage, only mounds created by substantial recharge farther from the channel are likely to
117 persist long enough to create seasonal time scale storage that results in meaningful local
118 increases in dry-season net stream gain (Cardenas, 2009; Nash *et al.*, 2018).

119 In this study, we explore the simulated influence of different BMR treatment designs in
120 various hydrogeologic settings. We used simulations of dynamic stream-aquifer systems in
121 MODFLOW to explore the general nature of effects to the groundwater system. The modeled
122 scenarios were inspired by the choices in BMR design frequently considered in the
123 intermountain western US and were implemented in the context of the different hydrogeologic

124 settings of stream corridors common in these systems. We focus on the influence of BMR on
125 alluvial aquifers in less constrained reaches of the fluvial corridor, where the effects of seasonal
126 variation in groundwater recharge from the stream or connected surface waters dominates over
127 the effects of variation in lateral recharge from hillslopes. In these systems, recharge from
128 surface waters at higher flows creates higher water tables and seasonally transient groundwater
129 mounds in the regions surrounding seasonal sources of recharge. This conceptualization
130 complements studies that have focused on the changes in lateral groundwater inflow due to
131 changes in stream stage for gaining streams (Nash et al., 2018) to extend understanding of the
132 effect of BMR treatments to settings where alluvial recharge originates predominantly from
133 stream-derived surface waters (Westbrook *et al.*, 2006) and to systems where streams are
134 generally losing.

135

136

METHODS

137

138

139

140

141

142

143

144

145

146

We developed MODFLOW groundwater models of hypothetical stream corridors to evaluate the general nature of hydrologic effects from varied BMR treatment designs in different hydrogeologic settings (fig. 1 and table 1). These models included the addition of a single BMS and various off-channel inundation scenarios. We recognize that most BMR treatments include the installation of several BMSs, but chose to focus on the mechanics of a single structure to aid in the fundamental scientific understanding necessary for effective management decisions involved with selecting BMR locations and designs. The potential for interactions between a sequence of structures to cause emergent, non-additive hydrologic behavior may be a useful direction for future research. Sensitivity analysis was used to evaluate how variations in site-specific hydrogeologic characteristics change the hydrologic effects of BMR treatments.

147 Numerical models were developed based on a simplified conceptual model of the effects
148 of BMR installations on an incised stream with a snowmelt dominated hydrograph, focusing on
149 settings where variation in groundwater recharge from the channel or channel-connected surface
150 waters are the dominant influence on storage in the alluvial aquifer. This setting is common for
151 stream restoration activities in the intermountain west of the United States, and modeling
152 scenarios in this setting were inspired by discussions with stream restoration practitioners in the
153 headwaters of the Missouri River in southwest Montana, USA. These simple models are not
154 intended to represent the absolute behavior or complexities of any single system or design, but
155 are intended to provide an understanding of the types of changes in groundwater dynamics that
156 might be expected.

157 The modeled scenarios were designed to evaluate how the addition of a single BMS to a
158 stream affects groundwater-mediated hydrologic connections through the fluvial corridor. Three
159 versions of each modeling scenario (fig. 1 and table 1) were developed to simulate differing
160 hydrogeologic settings, where the boundary conditions were defined to simulate a stream reach
161 that was generally gaining (G), losing (L), or strongly losing (SL) within the model domain.

162 *Conceptual Model*

163 Simulated fluvial corridors were based on streams with alluvial aquifers assumed to be 5-
164 20 m thick. Alluvial aquifers of this size are consistent with second to fourth-order streams in the
165 intermountain west, which also tend to be areas where natural beaver dams persist through high
166 flows (Macfarlane *et al.*, 2017). Floodplain soils that develop from overbank deposition are often
167 dominated by fine-grained deposits. However, the alluvial sediments that make up the aquifer are
168 typically composed of coarser-grained sands and gravels, due to the higher preservation potential
169 of coarse-grained sediments in a fluvial corridor (Aslan, 2013). Sand aquifers have saturated

170 hydraulic conductivities (K) ranging from about 10 to 100 m d⁻¹ (Heath, 1983). Bedrock
171 underlies the alluvium (fig. 2), and bedrock with limited secondary permeability normally has a K
172 value less than 1 m d⁻¹ (Heath, 1983).

173 For a given reach of the stream corridor, groundwater enters an alluvial aquifer from
174 upstream alluvium, and from uplands and bedrock along the lateral edges (Shaw *et al.*, 2014).
175 Our conceptual model focuses on areas where inflow from the upstream alluvium is typically
176 substantially higher than the lateral inputs. Groundwater can leave a reach of the corridor via
177 subsurface flow paths through the downstream alluvium. For the purpose of this study, we
178 assume alluvial groundwater loss to, or gain from, deeper regional aquifers are negligible.

179 Analysis of the seasonal storage generated by BMR requires a detailed understanding of
180 the dynamics of surface-subsurface exchange of water between the alluvial aquifer and surface
181 waters driven by differences in head. Streams often vary between gaining and losing over a range
182 of scales in both space and time (Niswonger and Prudic, 2005; Prudic, 1989; Winter *et al.*, 1998;
183 Woessner, 2000). We are considering streamflows and stream stage in settings with a snowmelt
184 driven hydrologic regime. In areas with relatively low lateral contributions like intermountain
185 basins, the associated seasonal changes in stream stage and the resulting potential for off-channel
186 floodplain inundation at higher flows are a primary control on groundwater recharge and the
187 formation of groundwater mounds.

188 Movement of water between the aquifer and atmosphere via precipitation and ET_{gw} may
189 also be important to understand the influence of BMR, particularly considering the potential for
190 increased water availability to plants. A common goal of BMR is to reestablish or expand the
191 riparian zone (Pilliod *et al.*, 2018). Where the water table is close to the land surface ET_{gw} can
192 supply much of the water used by wetland plants, and ET_{gw} can be a substantial portion of the

193 groundwater budget (Leake and Gungl, 2012). Local precipitation and snowmelt can provide
194 groundwater recharge when water is able to infiltrate through the vadose zone. Groundwater
195 recharge from this infiltration likely occurs during large precipitation events or snowmelt, but
196 under normal circumstances this contribution is small compared to other inputs to a reach control
197 volume.

198 Based upon this conceptual model, a finite volumetric groundwater budget for a control
199 volume of the alluvial aquifer (fig. 2) during a given period of time can be expressed as:

$$\begin{aligned} 200 \quad & G_{in-al} + G_{in-lat} + S_{in} + R = \\ 201 \quad & G_{out-al} + S_{out} + ET_{gw} + \Delta S \end{aligned} \quad (Eqn. 1)$$

202 where G_{in-al} and G_{out-al} are alluvial groundwater inflow and outflow; G_{in-lat} is lateral groundwater
203 inflow; S_{in} and S_{out} are groundwater recharge and discharge from/to surface waters; R is
204 groundwater recharge from local precipitation; ET_{gw} is groundwater evapotranspiration; and ΔS
205 is the change in the volume of water stored in the aquifer.

207 Net changes in storage (ΔS) at the same time of year over multi-year timescales are
208 expected to be near zero if there are no major alterations to the system (i.e. long-term dynamic
209 equilibrium). However, the potential to increase local storage of water that could then contribute
210 to dry-season streamflow within a given reach would necessarily arise from increasing the
211 seasonal amplitude of ΔS around zero. When ΔS is positive groundwater mounds form, and when
212 ΔS is negative these mounds dissipate. As the mounds dissipate the water is partitioned among
213 various outputs, such as water flowing to the stream (S_{out}), flowing out of the control volume as
214 groundwater (G_{out-al}), or being used for ET_{gw} .

215 *Baseline Numerical Models*

216 We used MODFLOW 2000 (Aquaveo, 2013; Harbaugh *et al.*, 2000) to construct simple,
217 yet spatially and temporally explicit, numerical groundwater flow models of alluvial aquifers
218 influenced by overlying surface waters. MODFLOW was developed by the USGS and is a
219 broadly applied numerical solution for groundwater head distributions. Modeling details,
220 including a discussion of model limitations and assumptions, such as how MODFLOW
221 addresses the nonlinear groundwater flow equation, are provided in Supporting Information.

222 The models were constructed to represent a reach of an alluvial aquifer 1,000 m long, 100
223 m wide, and 10 m thick (figs. 2 and 3). Aquifer properties were homogeneous and isotropic
224 throughout the model domain and were based on literature values for an unconfined coarse sand
225 aquifer ($K=25 \text{ m d}^{-1}$; specific yield (S_y)=0.2; (Fetter, 1994; Freeze and Cherry, 1979; Heath,
226 1983).

227 The models simulated transient hydrologic conditions over time and were run for 5 years
228 (1,826 days) using 261 weekly stress periods and daily computational time steps. In MODFLOW
229 “stress periods” are the feature that allows for non-steady-state modeling, such that boundary
230 conditions can vary among stress periods but are constant within a stress period.

231 Specified flux boundary conditions were used to simulate groundwater inflow through
232 the upstream alluvium, and along the lateral edges of the model domain to simulate hillslope
233 contributions (fig. 3). Alluvial inflow was at a constant $95 \text{ m}^3 \text{ d}^{-1}$ and lateral inflow was held
234 constant at $5 \text{ m}^3 \text{ d}^{-1}$ (fig. 4). These inflows were selected because they are reasonable given the
235 permeability of the aquifer, and they provided a slightly gaining stream in the gaining setting,
236 and a slightly losing stream for the losing setting. The rates were held constant because effects
237 due to changes in aquifer saturated thickness (and therefore transmissivity) and hydraulic
238 gradients at the edges of the model domain are anticipated to be slight relative to the effects from

239 the restoration. Constant external boundaries also allow an unconfounded perspective on storage
240 phenomena driven only by dynamic changes in stream stage and groundwater recharge from
241 surface waters within the model domain.

242 At the downstream end of the model domain, groundwater outflow was simulated using
243 the drain package (figs. 3 and 4) (Banta, 2000). Drains only remove water from the model
244 domain, and that only occurs when the groundwater elevation is higher than the drain elevation.
245 The amount of water that drains remove is determined by the difference between the
246 groundwater elevation and the drain elevation, and by a conductance term. We adjusted the drain
247 elevation to create models of stream reaches that were generally gaining, losing, or strongly
248 losing (Winter *et al.*, 1998) (Supporting Information table S1.1). The drain conductance was set
249 to $10 \text{ m}^2 \text{ d}^{-1}$, which provided for adequate groundwater outflow, and did not create flooding. For
250 these models, the drain conductance can be viewed as proportional to the alluvium's cross-
251 sectional transmissivity (i.e. the saturated cross sectional area of the alluvial aquifer times K ;
252 Käser and Hunkeler, 2016), so it represents the ease with which water can move down-valley
253 through the alluvial aquifer.

254 The STR stream package (Prudic, 1989) was used to simulate the bidirectional exchange
255 of water between stream channels and the alluvial aquifer (fig. 3). The STR package allows the
256 stream to be gaining water from or losing water to the aquifer depending on the relative elevation
257 of the stream surface (stage) and the groundwater elevation in each associated underlying cell.
258 The STR package includes simple channel hydraulic simulation that calculates the stream stage
259 based on the amount of stream discharge (e.g. $\text{m}^3 \text{ s}^{-1}$), the channel geometry, and Manning's
260 roughness coefficient (Barnes, 1967; Prudic, 1989). The annual streamflow hydrograph (fig. 5) at
261 the upstream end of the reach was identical for each modeled year, and was based on a simplified

262 symmetrical snowmelt driven stream hydrograph, with an average streamflow of 100 L s^{-1} , peak
263 flows of 420 L s^{-1} , and baseflows of 37 L s^{-1} . The top of the streambed was set 1 m below the
264 floodplain surface. The amount of water moving between the stream and the aquifer depends on
265 the difference in head between them, the streambed conductance, and the permeability of the
266 aquifer. We used a streambed conductance values of $0.5 \text{ m}^2 \text{ d}^{-1} \text{ m}^{-1}$ based on a vertical hydraulic
267 conductivity of a silt bottom ($K_{bed} = 0.5 \text{ m d}^{-1}$) because pools with fine-textured beds typically
268 cover a much greater proportion of the streambed than riffles in our study streams (see
269 Supporting Information, S1.1). The STR package does not simulate unsaturated flow, but we
270 considered this to be an appropriate simplification given that recharge occurs over several
271 months (fig. 5), and the depth to groundwater is only a few meters (Niswonger and Prudic,
272 2005).

273 Effects of ET_{gw} were not included in the modeling scenarios to allow for unconfounded
274 comparisons of the fundamental behavior of groundwater storage among simulations. However,
275 ET_{gw} was included in the sensitivity analysis to evaluate potential effects to the dynamic water
276 balance. More thorough exploration of the effects of evapotranspiration on the water balance
277 deserves its own effort, and is underway in parallel research. Groundwater recharge from local
278 precipitation was assumed to be negligible at the reach scale (Chen and Chen, 2003), as is typical
279 for semi-arid areas in southwest Montana, USA.

280 *Analysis Across BMR Scenarios*

281 The simulated influence of BMSs were added to the baseline MODFLOW models to
282 evaluate changes in model outputs. The model outputs of interest included groundwater recharge
283 from surface waters (gross stream loss), groundwater discharge to surface waters (gross stream
284 gains), net stream gains (gross stream gains minus gross stream loss), and down-valley

285 groundwater outflow. Groundwater level dynamics were also evaluated. Five BMR treatment
286 configurations were simulated in the gaining, losing, and strongly losing hydrogeological
287 settings to evaluate the implications of different BMR designs (table 1; figs. 1 and 3). These
288 treatments were inspired by designs used for BMR projects that we have monitored in southwest
289 Montana, USA. The treatments included installation of a BMS that creates: (1) an on-channel
290 pond (S), (2) an on-channel pond with seasonal reactivation of a side channel near the stream
291 (NC), (3) an on-channel pond with seasonal reactivation of a side channel further from the
292 stream (FC), (4) an on-channel pond with seasonal inundation of the floodplain (FI), and (5) an
293 on-channel pond with seasonal filling of an off-channel pond (OC).

294 The creation of an on-channel pond was a part of all treatment scenarios, and was
295 simulated by introducing a step in the slope of the streambed relative to the baseline
296 configuration. The upstream portion of the step had a relatively shallow slope to represent the
297 pool behind the BMS. At the bottom of the pool, the streambed dropped 1 m from one cell to the
298 next, to the level of the baseline, to represent the change in stream stage created at the location of
299 the BMS. While this approach simulates the change in stream stage (the boundary condition for
300 the groundwater model), it does not simulate the additional storage added to the surface-water
301 system due to the on-channel pond. For this study this approach is intended to simulate a BMS;
302 however, the effect would be similar for other topographic elements on the stream bed, such as
303 natural or constructed riffles.

304 Streamflow was routed into side channels for the NC, FC, and FI scenarios (figs. 1 and
305 3). Ten percent of streamflow was routed into the side channels when stream discharge was
306 greater than 40 L/s. This configuration resulted in side-channel activation for 19 weeks each
307 year, from mid-April to early-August (fig. 5). The conductance of the stream bed sediments for

308 the side channels was simulated as being the same as the main channel. Since various
309 conceptualizations could be used to justify both higher and lower values, we believe that this is
310 an appropriate simplification.

311 The influence of an off-channel pond for the OC scenario (figs. 1 and 3) was simulated
312 using the head-dependent boundary condition implemented in MODFLOW's river package
313 (Harbaugh *et al.*, 2000). The river package simulates groundwater/surface-water exchange
314 almost identically to the stream package (Brunner *et al.*, 2009), except channel hydraulics are not
315 simulated and the stage is explicitly defined in the river package. We conceptualized the pond as
316 a floodplain depression that is filled when a side channel is activated during high flows in the
317 spring. After filling, the stage in the pond decreased until mid-September, at which point the
318 pond went dry and thus ceased to provide recharge. The change in pond stage over the summer
319 was based on the simulated loss to infiltration (recharge to the aquifer) and reasonable rates of
320 open-water evaporation, given a pond approximately 30 m wide by 200 m long, and with 600
321 mm yr⁻¹ of evaporation. Off-channel ponds, or groups of ponds, of this size are common features
322 of natural beaver complexes (e.g. see Wegener *et al.*, 2017). To maintain conservation of mass in
323 the water budget, calculated streamflows were reduced at the start of snowmelt by the amount of
324 water that is needed to account for the total annual infiltration and evaporation from the pond.
325 Filling the pond required between 8.5 and 12.6% of streamflow for one week in the early spring,
326 depending on the setting.

327 *Assessing Independent Parameter Sensitivity for the Far Channel Scenario*

328 The influence of different hydrologic parameters on the inferred effects of BMR on
329 groundwater storage dynamics was evaluated by independently perturbing parameter values for
330 aquifer K , aquifer S_y , streambed conductance, and drain conductance in the baseline and far

331 channel (FC) scenarios in each of the hydrogeologic settings. The FC scenario was used since
332 provided the largest influence of the non-off-channel pond scenarios, and therefore was
333 reasonably representative of most BMR treatments. ET_{gw} was also added to the model to provide
334 a cursory evaluation of its potential importance to the water balance.

335 Each of the tested parameters was varied within realistic values for the northern Rocky
336 Mountains of the United States. The tested K and S_y values were appropriate for unconsolidated
337 sediments from silt to gravel (Heath, 1983). In most unconsolidated sediments S_y and K are
338 related by the pore structure of the sediment (Heath, 1983); however, we treated S_y and K as
339 independent parameters in this sensitivity analysis to assess their unique influences. The stream-
340 bed conductance values represent streams with the same geometry, but with bed sediments
341 ranging from clay to sandy gravel. The drain conductance value influences the rate at which
342 water discharges from the downgradient model boundary, and so represent settings ranging from
343 a downstream constriction (e.g. a bedrock notch) to a downstream reach with a thicker and wider
344 accumulation of high permeability sediments. Tested maximum ET_{gw} rates (ET_{max}) were based
345 on literature values for bare soil to dense willow stands, and the evapotranspiration extinction
346 depth (ET_{XD}) was based on values from grass to trees in soils ranging from silty-clay loam to
347 sand (Johns, 1989; Lautz, 2008; Leenhouts *et al.*, 2005; Persson, 1995; Scott *et al.*, 2004; Shah *et*
348 *al.*, 2007).

349 The primary criterion used to compare the sensitivities of simulated storage dynamics to
350 variation in parameter values was the difference in net stream gain between the baseline and FC
351 model in mid-August of the 4th model year (stress period 240). Changes in groundwater
352 recharge from surface waters and groundwater discharge to surface waters were also evaluated
353 for stress period 240, and are included in the Supporting Information (sections S2.3 and S2.4).

354 This first-order approach only provides information about the independent influence of the
355 parameter values tested, and does not include interactions between parameters. Sensitivity
356 analysis is discussed in greater detail in Supporting Information (section S2).

357

358

RESULTS

359

360

361

362

363

364

365

366

367

368

Simulation results provide a heuristic illustration of how general patterns in the groundwater budget components and the head distribution in the aquifer respond to different BMS strategies. To evaluate the effects of BMR on the annual groundwater budget, we focused on summary statistics for model year 4 (the last year modeled), and effects during the dry season were evaluated over a week in mid-August of year 4 (stress period 240). Comparisons of differences in summary statistics relative to the baseline model provide perspective on the influence of BMR on hydrologic patterns driven by design choices, and how these patterns differ in systems where the stream is gaining, losing, or strongly losing. The sensitivity analysis provides perspective on the relative influence of site-specific hydrologic properties on the nature of the alluvial aquifer's response to restoration.

369

BMR Scenarios

370

371

372

373

374

375

376

While this exercise was hypothetical in nature and does not reflect the complexity of a real stream, the use of deterministic models under controlled conditions generates data that allow calculation of metrics that directly reflect how a restored stream might be expected to differ from its unrestored condition in terms of its interactions with the alluvial aquifer, even when the effects of a single BMS are more subtle than could be measured in the field. Hence, these modeling results represent general patterns in the hydrologic response that would be expected from common decisions regarding BMR design in differing hydrogeologic settings.

377 **Recharge from Gross Stream Loss.** All BMS treatment types in all settings caused
378 groundwater recharge from gross stream loss within the model domain to increase, both on an
379 annual basis and during the dry season (tables 2 and 3; figs. 6a and b). In general, the results
380 showed that the change in recharge from surface waters was lowest in the strongly losing stream
381 setting, and greatest in the gaining stream setting. This pattern reflects how treatments cause
382 portions of the stream to become more strongly losing, and that shift is most pronounced when
383 that portion of the stream was gaining prior to treatment. For all settings the OC treatment
384 resulted in the smallest change in gross stream loss (figs. 6a and b).

385 **Discharge to Gross Stream Gain.** Similar to the effects on gross stream loss, gross
386 stream gain from groundwater within the model domain increased for most treatments in all
387 settings, both on an annual basis and during the dry season (tables 2 and 3; fig. 6). These
388 increases were largely proportional to the increases in gross stream loss (figs. 6a and 6b). The
389 OC treatment resulted in the smallest change in gross stream gain for all settings (fig. 6).

390 **Net Stream Gain.** All BMR treatments in all settings caused a reduction in the average
391 annual net stream gain (fig. 6c). While the increased gross stream losses were partly offset by
392 increased gross stream gains after treatment, the net effect on an annual basis was for the stream
393 to lose more water to the aquifer (figs. 6c and 7), which was balanced in the water budget
394 primarily by increases in subsurface down-valley flow, as discussed below.

395 Model results during the dry season were markedly different from the annual average
396 results (figs. 6c, 6d and 7). All BMR treatments in the gaining and losing settings resulted in
397 increases in dry-season net stream gains (table 3), with the OC treatment causing the largest
398 increase. In the strongly losing setting, all treatments other than OC resulted in decreased net
399 stream gains (table 3). The largest of these simulated increases represented a 0.4% increase in

400 mid-August stream flow, which would be immeasurably small from a field perspective.

401 **Down-Valley Groundwater Outflow.** All treatment types in all settings resulted in an
402 increase in groundwater outflow from the downstream end of the model domain (tables 2 and 3),
403 balancing the decreases in net stream gain. These increases were similar in the gaining and losing
404 stream settings. In the strongly losing stream setting, groundwater outflows increases were
405 greater. The OC treatments in all settings resulted in groundwater outflow increases 1.4 to 3.1
406 times greater than the other treatments (tables 2 and 3).

407 **Groundwater Levels.** For all BMR scenarios groundwater mounds formed in recharge
408 zones during high flows and then dissipated as they drained to various outputs during lower
409 flows. The groundwater mound created by the in-stream structure persisted throughout the year,
410 but expanded and contracted with flow (e.g. fig. 8a). The additional groundwater mounding
411 created by seasonal off-channel inundation (NC, FC, and FI) dissipated rapidly once baseflow
412 was reached. This rapid dissipation caused the S, NC, FC, and FI scenarios to all result in similar
413 changes to dry-season groundwater levels (e.g. fig. 8b). Mid-August groundwater levels near the
414 upstream and downstream ends of the model domain showed slight changes while groundwater
415 levels near and immediately upstream of the BMS and off-channel pond showed more
416 pronounced increases (table 3 and fig. 8b).

417 The simulated changes in groundwater levels relative to baseline ranged up to 78 cm.
418 These values in are similar to those reported in other studies (Bouwes *et al.*, 2016; Janzen and
419 Westbrook, 2011; Majerova *et al.*, 2015; Pollock *et al.*, 2018; Westbrook *et al.*, 2006).
420 Monitoring results from BMR projects associated with our field studies in southwestern Montana
421 also demonstrate a similar response, with maximum observed changes in groundwater levels
422 after BMS installations of about 60 cm (fig. S3.1).

423 **Change in annual head amplitude.** The amount of water stored within the unconfined
424 alluvial aquifer and then released on an annual basis will be related by specific yield (S_y) to the
425 spatially-aggregated amplitude of annual mounding. To measure this model output we compared
426 the volume of storage between minimum and maximum heads for each cell during model year 4.
427 For all scenarios other than OC, the simulated changes in average amplitude of groundwater
428 hydrographs due to the addition of BMSs were similar within each hydrogeologic setting (table
429 2). In the gaining models the amplitude increased, indicating that more water was stored and then
430 released from the aquifer within the model domain each year. The losing models showed a
431 decrease in amplitude due to a less variable stream stage near the BMS (fig. 8c). The strongly
432 losing models showed only modest increases or decreases in the amplitude. In all hydrologic
433 settings the OC scenario resulted larger changes in storage amplitudes than the other scenarios.

434 *Sensitivity Analysis*

435 The sensitivity analysis of the FC treatment scenario allows comparisons of the relative
436 influence of reasonable variation in different model parameters on local alluvial groundwater
437 storage behavior. Even though changes in dry-season net stream gains were negligible compared
438 to stream flows, we explore variation in this response variable as a useful comparative summary
439 metric of local seasonal storage behavior. Changes in gross stream loss and gross stream gain
440 which results from the sensitivity analysis are also included in Supporting Information (tables
441 S2.2 and S2.3).

442 With respect to the range of parameter values selected for the sensitivity analysis, dry-
443 season net stream gains were most sensitive to the changes in the K of the aquifer, S_y of the
444 aquifer, and ET_{max} values (table 4). Variation in streambed conductance and drain conductance
445 had the least influence (table 4). The greatest simulated increase in dry-season net stream gain

446 due to a single BMS during the sensitivity analysis was $10.7 \text{ m}^3 \text{ d}^{-1}$ (0.12 L s^{-1}), while the
447 greatest decrease was $-31.5 \text{ m}^3 \text{ d}^{-1}$ (-0.36 L s^{-1}) (table 4).

448 In all settings, the greatest increase in late-summer net stream gains due to the FC
449 treatment occurred at the intermediate K value of 2.5 m d^{-1} , which would be representative of a
450 silty sand (Heath, 1983). K values less than 2.5 m d^{-1} caused net stream gains to be lower and
451 caused the models to be less sensitive to the hydrogeologic setting (table 4), while K values
452 greater than 2.5 m d^{-1} caused the net stream gains to be lower and caused the models to be more
453 sensitive to the hydrogeologic setting (table 4).

454 In all hydrogeologic settings, the change in net stream gains was larger with higher S_y ,
455 and smaller with lower S_y (table 4). When S_y was 0.02 (the lowest value tested) the FC treatment
456 resulted in decreased dry-season net stream gains in all hydrogeologic settings. When S_y values
457 were 0.3 or 0.4 the FC treatment resulted in increased dry-season net stream gains in all
458 hydrogeologic settings.

459 The model results were least sensitive to streambed conductance and drain conductance.
460 However, the differences in the influence of BMR among hydrologic settings were less
461 pronounced when low conductance terms were used (table 4).

462 When ET_{gw} was added to the gaining and losing stream models, a direct and linear
463 decrease in dry-season net stream gain emerged as the maximum ET rate (ET_{max}) increased
464 (ET_{XD} was held at 2 m; table 4). The strongly losing stream model responded similarly up to 600
465 mm yr^{-1} , but at 1200 mm yr^{-1} , the effect was lower than would result from a linear relationship
466 since the groundwater level was held near the extinction depth. The simulation where ET_{max} was
467 600 mm yr^{-1} and ET_{XD} was 1 m resulted in little effect on model predictions compared to models
468 without ET simulation since that extinction depth is near the typical depth to groundwater.

469 Increasing ET_{XD} to 2 m resulted in a noticeable decrease in simulated dry-season net stream
470 gains; however, further increases in extinction depth resulted in little additional influence.
471 Regardless of setting, when ET_{max} was 300 mm yr⁻¹ or greater (with an ET_{XD} of 2 m), or when
472 ET_{XD} was 2 m or greater (with ET_{max} at 600 mm yr⁻¹), the effect of the treatment was a decrease
473 in dry-season net stream gains.

474 DISCUSSION

475 Results from modeling the effects of different BMR design choices provide a basis for
476 understanding the general types of groundwater-mediated influences that should be expected
477 from common restoration activities. These effects are modified depending on site-specific
478 hydrologic characteristics. Together this information is useful for developing site-selection
479 strategies and restoration designs that are likely to meet project objectives.

480 While this study focused on BMR, the hydrologic patterns illustrated by these modeling
481 exercises also provide insight into the effects of streambed topography and intermittent off-
482 channel streamflows on hydrologic storage in the fluvial corridor. Increased access to the
483 floodplain is an objective in many types of stream restoration, and the potential effects from
484 floodplain inundation are important in many stream corridors.

485 *Influences of different BMR designs*

486 Changes in the bidirectional movement of water between the stream and the aquifer is the
487 predominant driver of groundwater-mediated influences from BMR. Installing a BMS directly
488 causes higher stream stage above the structure, and adjacent groundwater levels rise until a new
489 dynamic equilibrium is established. When BMR treatment designs include intermittent flow
490 through side channels, or floodplain inundation, the geographic pattern of groundwater recharge
491 is also altered. Our modeling (using 1 m tall BMSs) showed increases in groundwater levels by

492 up to 78 cm, which is similar to values reported in other studies (Bouwes *et al.*, 2016; Janzen and
493 Westbrook, 2011; Majerova *et al.*, 2015; Pollock *et al.*, 2018; Westbrook *et al.*, 2006), and to
494 values we have observed during our field studies in southwestern Montana.

495 The response time of seasonal dynamic storage is determined by the response of the
496 hydrologic system to an excitation in hydraulic head (i.e., mechanical energy) in areas of
497 recharge, and the subsequent dissipation of the resulting groundwater mound. Interpreting
498 seasonal dynamics of groundwater mounding provides perspective on how the spatiotemporal
499 distribution of groundwater discharge to a stream responds to the alteration of hydraulic
500 gradients created by increased groundwater recharge during high streamflows. The time that it
501 takes for a groundwater mound to dissipate explains the magnitude of dry-season effects from
502 different BMR treatments. The rate of mound dissipation is directly related to the transmissivity
503 of the aquifer. Rapid dissipation of mounds for our scenario testing (with aquifer K values of 25
504 m d⁻¹) explains why all treatment scenarios in our models without off-channel ponding had
505 similar effects on dry-season net stream gains and suggests that in many settings the persistence
506 of groundwater mounds may be more important than the spatial distribution of recharge.

507 Regardless of the BMS type, the ubiquitous consequences of simulated restoration
508 included increased recharge to groundwater (gross stream loss) and increased down-valley
509 groundwater outflow. This suggests the potential for BMR treatments to create storage that
510 extends beyond the treatment reach, which may represent influence beyond seasonal time scales.
511 Depending on the geometry of the downstream aquifer, the increase in groundwater outflow may
512 lead to larger spatial scale, and longer time scale, flow paths that discharge to outputs such as
513 stream gains and evapotranspiration.

514 Simulated enhancement of seasonal groundwater mounding created by periodic off-

515 channel inundation illustrates the need for conceptual models of fluvial corridors that incorporate
516 a wider array of variably saturated flow paths. For example, the “gill-lung” analogy (Sawyer *et*
517 *al.*, 2009) provides for unidirectional movement of water from groundwater to the stream (gill),
518 or variably saturated bidirectional movement of water between the stream and its banks (lung);
519 however, intermittently active subsurface flow paths sourced from periodic inundation by surface
520 waters are both variably saturated and unidirectional. This may also represent a hot spot of
521 biogeochemical influence on water quality driven by episodic transport and alternation between
522 aerobic and anaerobic processes (Boano, *et al.*, 2014; McClain *et al.*, 2003). This work supports
523 building evidence that the evolution of hyporheic conceptual models to a more holistic fluvial
524 corridor science needs to include transient hyporheic flow paths that are driven by recharge from
525 periodic inundation, which may borrow traits from both gills and lungs (Sawyer *et al.*, 2009;
526 Ward and Packman, 2019). Holistic models will also need to account for the associated dynamics
527 of both water and energy movement on stream subsurface exchange along fluvial corridors (e.g.
528 dynamic storage age selection models, Harman *et al.*, 2016).

529 *Influences of site characteristics*

530 The results of the sensitivity analysis aid in selecting sites with the appropriate
531 hydrogeologic properties for achieving restoration objectives. The sensitivity analysis suggested
532 that variation in hydraulic conductivity (K), specific yield (S_y), and groundwater
533 evapotranspiration (ET_{gw}) are important considerations in restoration design, because
534 independent variation in these characteristics drove more variation in groundwater storage
535 dynamics than stream bed or drain conductance.

536 Intermediate K values (as for a silty-sand) provided the greatest increase in late-summer
537 streamflows due to striking a balance between allowing more recharge and providing longer

538 storage times. Models with lower K values had groundwater mounds that dissipated more slowly,
539 but the magnitude of the flow was less. For models with higher K values the groundwater
540 mounds dissipated too rapidly to maintain seasonal time scale storage. At sites with relatively
541 high K values increasing the distance between the area of off channel inundation and the stream
542 could be used to maintain seasonal time scale storage, but in most stream restoration projects, the
543 distance that water can be diverted using gravity will limit the location of recharge to the
544 floodplain.

545 Larger S_y values allow a larger volume of water to be stored in the aquifer for a given
546 change in head, and the change in head is strongly influenced by the change in stream stage
547 created by the BMS. In general, S_y increases with grain size due to increased drainage capacity of
548 the courser substrates, so values for clays are quite low while values for gravel and cobbles are
549 high. Since S_y and K are typically related, a balance is needed between maximizing storage
550 volume (course sediments) and providing the intermediate K values discussed above.

551 The trade-off between dry-season net stream gains and ET_{gw} showed that ET_{gw} may cause
552 the influence of aquifer storage to be reduced when higher groundwater levels allow for higher
553 ET_{gw} . These effects would be less pronounced if pretreatment depth to groundwater was shallow
554 since the plants would not be water limited prior to treatment. Similarly, higher ET_{gw} would be
555 negligible if post-treatment groundwater levels and capillary zones were below the root depth.
556 Sensitivity analyses of evapotranspiration rates provide a general demonstration of how
557 evapotranspiration and net stream gains are in direct competition for stored groundwater (Chen
558 and Chen, 2003). In many cases, this competition caused simulated treatments that would have
559 otherwise increased net stream gains to show a decrease instead, similar to the results of Nash et
560 al. (2018).

561 The sensitivity analysis also demonstrated how the hydrogeologic setting (net gaining,
562 losing, or strongly losing) may not always be a critical influence on the changes in groundwater
563 recharge regimes resulting from BMR. Differences in the gaining or losing nature of the stream
564 had little influence on simulated dry-season net stream gain when K was low, when drain
565 conductance was low, or when streambed conductance was either high or low (table 4). The lack
566 of an effect with lower K , lower drain conductance, and higher streambed conductance all
567 suggest that when water can flow to the stream much more easily than it can flow through the
568 aquifer, the water will flow to the stream regardless of setting. The results with low streambed
569 conductance values showed that the opposite is also true; when it is difficult for water to flow to
570 the stream, it will flow out through the aquifer instead. Thus, while the overall gaining or losing
571 nature of a stream is an important characteristic of the fluvial corridor, it cannot be used in
572 isolation to anticipate how the system will respond to restoration activities. Instead, the character
573 of the fluvial corridor needs to be evaluated holistically (Ward and Packman, 2019).

574 *Considerations for achieving restoration objectives*

575 The restoration objectives and the site conditions should guide the restoration design.
576 Objectives for a BMR project may include increasing the extent and vigor of riparian vegetation
577 (increased ET_{gw} in the treatment area), increasing dry-season net stream gains in the treatment
578 area, or increasing groundwater outflow through the subsurface of the fluvial corridor (Pilliod *et*
579 *al.*, 2018). All of these objectives will require an increase in groundwater recharge, but it is the
580 partitioning of that water among these different outputs that will determine if project objectives
581 are met. While each of these objectives are individually worthwhile, their achievement is
582 inherently mutually limited because they are competing for the enhanced recharge (eqn. 1).

583 To increase the extent and vigor of the riparian vegetation the priority should be to

584 increase groundwater elevation in the root zone over as large an area as possible. An aquifer with
585 a relatively low K , such as a silt, is more likely to meet this objective since groundwater mounds
586 would dissipate slowly. These areas may require several years to become saturated due to the
587 movement of water being limited by the low K , but once they are saturated, they will hold the
588 water for longer following high streamflows. A fine substrate, such as would exist in historical
589 wetlands, would also likely be more suitable for the viability of planted riparian vegetation (e.g.,
590 willows, Castro-Morales *et al.*, 2014).

591 To increase dry-season net stream gains in the area near the treatment, BMR design
592 should promote increased recharge during high streamflows that increase the extent, magnitude,
593 and duration of groundwater mounds that can drive discharge to the stream through the dry
594 season. The persistence of groundwater mounds will depend on the distance between
595 groundwater recharge and the stream, the transmissivity of the aquifer, and the duration of
596 recharge. For our models, treatments that included off-channel ponds provided the greatest
597 influence since the groundwater mounds associated with them remained fully formed through the
598 dry season. Sites with a substrate composed of silty sand also provided the greatest increase in
599 dry-season net stream gains. Treatment reaches upstream of bedrock notches (low drain
600 conductance), where down-valley groundwater flow would be limited, would also promote
601 increases in net stream gain within the treatment reach. Even in ideal settings, a single BMS is
602 unlikely to meaningfully influence local streamflow.

603 When the objective of the BMR treatment is to increase long-term average streamflows
604 over areas larger than the treatment reach the design should focus on increasing groundwater
605 outflow to contribute to higher heads over a more extensive aquifer area. The most groundwater
606 outflow will occur at sites where the most gross stream loss occurs and where that water can

607 easily flow through the aquifer at a depth where it is less accessible to plants. That is, sites with
608 strongly losing streams, high permeability aquifer materials, and an unrestricted groundwater
609 flow path down gradient (e.g. an open valley without bedrock notches).

610

611

CONCLUSIONS

612 The groundwater-mediated effects of BMR will vary based on the hydrogeologic
613 characteristics of the treated site and the treatment design. The results of this modeling exercise
614 illustrate important considerations for site selection and BMR design relative to project
615 objectives. The simulated groundwater-mediated changes in net stream gain within the treatment
616 reach due to a single BMS were immeasurably small compared to streamflow, and higher
617 evapotranspiration of groundwater caused decreases in simulated dry-season net stream gains in
618 many settings. However, all simulated BMR treatments caused increases in groundwater
619 recharge that elevated groundwater levels near the BMS and increased down-valley groundwater
620 outflow from the treated reach. Increased down-valley groundwater outflow may ultimately
621 increase larger-scale groundwater storage that results in increased flows downstream of the
622 restoration site.

623

624

625

ACKNOWLEDGEMENTS

626 This work was funded through a Montana Water Center faculty seed grant, The Nature
627 Conservancy – Montana, the Montana Department of Natural Resources and Conservation, and
628 the Montana Agricultural Experiment Station (USDA NIFA MSU CoA MAES MONB00349).
629 The Montana Bureau of Mines and Geology, and particularly Ginette Abdo, provided support for

630 this work. Detailed discussions with Montana stream restoration practitioners, including Nathan
631 Korb (The Nature Conservancy), Scott Gilliland (Gilliland Associates), Karin Boyd (Applied
632 Geomorphology), and Amy Chadwick (Great West Engineering) helped to guide this work.
633 Additional funding and ideas from the Montana NSF EPSCoR Consortium for Research on
634 Environmental Water Systems (CREWS, NSF EPSCoR OIA-1757351) was critical in
635 preparation of this manuscript. Any opinions, findings, and conclusions or recommendations
636 expressed in this material are those of the authors and do not necessarily reflect the views of the
637 National Science Foundation. Finally, we thank the editors and anonymous reviewers for
638 thoughtful comments that helped to improve and clarify this manuscript.

639

640

DATA AVAILABILITY

641 The three baseline models and the 15 models for the treatment scenarios (table 1 of the
642 main text) are publicly available through the HydroShare database:

643 <http://www.hydroshare.org/resource/d3b23a5e59cb408c8953b6eff2ee7b73>

644

LITERATURE CITED

- 646 Aquaveo, 2013. Groundwater Modeling System (GMS), v. 9.2. <https://www.aquaveo.com/> [accessed
647 6/19/22].
- 648 Aslan, A., 2013. Fluvial Environments. S. A. Elias (Editor). Encyclopedia of Quaternary Science.
649 Elsevier, pp. 663–675. <https://doi.org/10.1016/B978-0-444-53643-3.09988-X>
- 650 Banta, E.R., 2000. MODFLOW-2000, the U.S. Geological Survey Modular Ground-Water Model;
651 Documentation of Packages for Simulating Evapotranspiration with a Segmented Function (ETS1)
652 and Drains with Return Flow (DRT1). U.S. Geological Survey Open-File Report 00-466.
653 <https://pubs.er.usgs.gov/publication/ofr00466>
- 654 Barnes, H.H., 1967. Roughness Characteristics of Natural Channels. U.S. Geological Survey Water-
655 Supply Paper 1849. <https://pubs.er.usgs.gov/publication/wsp1849>
- 656 Barnett, T.P., J.C. Adam, and D.P. Lettenmaier, 2005. Potential Impacts of a Warming Climate on Water
657 Availability in Snow-Dominated Regions. *Nature* 438:303–309.
658 <https://doi.org/10.1038/nature04141>
- 659 Berghuijs, W.R., R.A. Woods, and M. Hrachowitz, 2014. A Precipitation Shift from Snow towards Rain
660 Leads to a Decrease in Streamflow. *Nature Climate Change* 4:583–586.
661 <https://doi.org/10.1038/NCLIMATE2246>
- 662 Boano, F., J.W. Harvey, A. Marion, A.I. Packman, R. Revelli, L. Ridolfi, and A. Wörman, 2014.
663 Hyporheic Flow and Transport Processes: Mechanisms, Models, and Biogeochemical Implications.
664 *Reviews of Geophysics* 52:603–679. <https://doi.org/10.1002/2012RG000417>
- 665 Boutt, D.F. and B.J. Fleming, 2009. Implications of Anthropogenic River Stage Fluctuations on Mass
666 Transport in a Valley Fill Aquifer. *Water Resources Research* 45:1–14.
667 <https://doi.org/10.1029/2007WR006526>
- 668 Bouwes, N., N. Weber, C.E. Jordan, W.C. Saunders, I.A. Tattam, C. Volk, J.M. Wheaton, and M.M.
669 Pollock, 2016. Ecosystem Experiment Reveals Benefits of Natural and Simulated Beaver Dams to a
670 Threatened Population of Steelhead (*Oncorhynchus Mykiss*). *Scientific Reports* 8:1–12.
671 <https://doi.org/10.1038/srep28581>
- 672 Bredehoeft, J.D., 2002. The Water Budget Myth Revisited: Why Hydrogeologists Model. *Groundwater*
673 40:340–345. <https://doi.org/10.1111/j.1745-6584.2002.tb02511.x>
- 674 Bredehoeft, J.D., S.S. Papadopoulos, and H.H. Cooper, 1982. Groundwater: The Water Budget Myth. *in*
675 *Scientific Basis of Water Resource Management*:51–57. <https://doi.org/10.2172/7166138>
- 676 Brunner, P., P.G. Cook, and C.T. Simmons, 2009. Hydrogeologic Controls on Disconnection between
677 Surface Water and Groundwater. *Water Resources Research* 45:1–13.
678 <https://doi.org/10.1029/2008WR006953>
- 679 Burns, D.A. and J.J. McDonnell, 1998. Effects of a Beaver Pond on Runoff Processes: Comparison of
680 Two Headwater Catchments. *Journal of Hydrology* 205:248–264. [https://doi.org/10.1016/S0022-
681 1694\(98\)00081-X](https://doi.org/10.1016/S0022-1694(98)00081-X)
- 682 Cardenas, M.B., 2008. The Effect of River Bend Morphology on Flow and Timescales of Surface Water-
683 Groundwater Exchange across Pointbars. *Journal of Hydrology* 362:134–141.
684 <https://doi.org/10.1016/j.jhydrol.2008.08.018>

685 Cardenas, M.B., 2009. Stream-Aquifer Interactions and Hyporheic Exchange in Gaining and Losing
686 Sinuous Streams. *Water Resources Research* 45:1–13. <https://doi.org/10.1029/2008WR007651>

687 Cardenas, M.B., J.L. Wilson, and V.A. Zlotnik, 2004. Impact of Heterogeneity, Bed Forms, and Stream
688 Curvature on Subchannel Hyporheic Exchange. *Water Resources Research* 40:1–14.
689 <https://doi.org/10.1029/2004WR003008>

690 Castro-Morales, L.M., P.F. Quintana-Ascencio, J.E. Fauth, K.J. Ponzio, and D.L. Hall, 2014.
691 Environmental Factors Affecting Germination and Seedling Survival of Carolina Willow (*Salix*
692 *Caroliniana*). *Wetlands* 34:469–478. <https://doi.org/10.1007/s13157-014-0513-6>

693 Cayan, D.R., S.A. Kammerdiener, M.D. Dettinger, J.M. Caprio, and D.H. Peterson, 2001. Changes in the
694 Onset of Spring in the Western United States. *Bulletin of the American Meteorological Society*
695 82:399–415. [https://doi.org/10.1175/1520-0477\(2001\)082<0399:CITOOS>2.3.CO;2](https://doi.org/10.1175/1520-0477(2001)082<0399:CITOOS>2.3.CO;2)

696 Chen, X. and X. Chen, 2003. Stream Water Infiltration, Bank Storage, and Storage Zone Changes Due to
697 Stream-Stage Fluctuations. *Journal of Hydrology* 280:246–264. [https://doi.org/10.1016/S0022-1694\(03\)00232-4](https://doi.org/10.1016/S0022-1694(03)00232-4)

699 Clow, D.W., 2010. Changes in the Timing of Snowmelt and Streamflow in Colorado: A Response to
700 Recent Warming. *Journal of Climate* 23:2293–2306. <https://doi.org/10.1175/2009JCLI2951.1>

701 Fetter, C.W., 1994. *Applied Hydrogeology*. Prentice Hall, Upper Saddle River, NJ. ISBN 9780023364907

702 Freeze, R.A. and J.A. Cherry, 1979. *Groundwater*. Prentice-Hall Inc, Englewood Cliffs, NJ. ISBN
703 9780133653120

704 Gomez-Velez, J.D., J.L. Wilson, M.B. Cardenas, and J.W. Harvey, 2017. Flow and Residence Times of
705 Dynamic River Bank Storage and Sinuosity-Driven Hyporheic Exchange. *Water Resources*
706 *Research* 53:8572–8595. <https://doi.org/10.1002/2017WR021362>

707 Gurnell, A.M., 1998. The Hydrogeomorphological Effects of Beaver Dam-Building Activity. *Progress in*
708 *Physical Geography* 22:167–189. <https://doi.org/10.1177%2F030913339802200202>

709 Harbaugh, A.W., E.R. Banta, M.C. Hill, M.G. McDonald, and C.G. Groat, 2000. MODFLOW-2000, The
710 U. S. Geological Survey Modular Ground-Water Model User Guide to Modularization Concepts
711 and the Ground-Water Flow Process. U.S. Geological Survey Open-File Report 00–92.
712 <https://pubs.er.usgs.gov/publication/ofr200092>

713 Harman, C.J., A.S. Ward, and A. Ball, 2016. How Does Reach-Scale Stream-Hyporheic Transport Vary
714 with Discharge? Insights from rSAS Analysis of Sequential Tracer Injections in a Headwater
715 Mountain Stream. *Water Resources Research* 52:7130–7150.
716 <https://doi.org/10.1002/2016WR018832>

717 Harvey, J.W. and K.E. Bencala, 1993. The Effect of Streambed Topography on Surface-Subsurface Water
718 Exchange in Mountain Catchments. *Water Resources Research* 29:89–98.
719 <https://doi.org/10.1029/92WR01960>

720 Harvey, J.W., J.D. Gomez-Velez, N.M. Schmadel, D. Scott, E. Boyer, R. Alexander, K. Eng, H. Golden,
721 A. Kettner, C. Konrad, R. Moore, J. Pizzuto, G. Schwarz, C. Soulsby, and J. Choi, 2019. How
722 Hydrologic Connectivity Regulates Water Quality in River Corridors. *Journal of the American*
723 *Water Resources Association* 55:369–381. <https://doi.org/10.1111/1752-1688.12691>

724 Heath, R.C., 1983. *Basic Ground-Water Hydrology*. U.S. Geological Survey Water-Supply Paper 2220.
725 <https://pubs.er.usgs.gov/publication/wsp2220>

- 726 Helton, A.M., G.C. Poole, R.A. Payn, C. Izurieta, and J.A. Stanford, 2014. Relative Influences of the
727 River Channel, Floodplain Surface, and Alluvial Aquifer on Simulated Hydrologic Residence Time
728 in a Montane River Floodplain. *Geomorphology* 205:17–26.
729 <https://doi.org/10.1016/j.geomorph.2012.01.004>
- 730 Hunt, L.J.H., J. Fair, and M. Odland, 2018. Meadow Restoration Increases Baseflow and Groundwater
731 Storage in the Sierra Nevada Mountains of California. *Journal of the American Water Resources*
732 *Association* 54:1127–1136. <https://doi.org/10.1111/1752-1688.12675>
- 733 Janzen, K. and C.J. Westbrook, 2011. Hyporheic Flows Along a Channelled Peatland: Influence of
734 Beaver Dams. *Canadian Water Resources Journal / Revue Canadienne Des Ressources Hydriques*
735 36:331–347. <https://doi.org/10.4296/cwrj3604846>
- 736 Johns, E.L.(Editor), 1989. *Water Use by Naturally Occurring Vegetation including an annotated*
737 *bibliography*. American Society of Civil Engineers, New York. ISBN 0-87262-732-2
- 738 Kasahara, T. and S.M. Wondzell, 2003. Geomorphic Controls on Hyporheic Exchange Flow in Mountain
739 Streams. *Water Resources Research* 39:1005. <https://doi.org/10.1029/2002WR001386>
- 740 Kasahara, T. and A.R. Hill, 2006. Hyporheic Exchange Flows Induced by Constructed Riffles and Steps
741 in Lowland Streams in Southern Ontario, Canada. *Hydrological Processes* 20:4287–4305.
742 <https://doi.org/10.1002/hyp.6174>
- 743 Käser, D. and D. Hunkeler, 2016. Contribution of Alluvial Groundwater to the Outflow of Mountainous
744 Catchments. *Water Resources Research* 52:680–697. <https://doi.org/10.1002/2014WR016730>
- 745 Kendy, E. and J.D. Bredehoeft, 2006. Transient Effects of Groundwater Pumping and Surface-Water-
746 Irrigation Returns on Streamflow. *Water Resources Research* 42:1–11.
747 <https://doi.org/10.1029/2005WR004792>
- 748 Klein, L.R., S.R. Clayton, J.R. Alldredge, and P. Goodwin, 2007. Long-Term Monitoring and Evaluation
749 of the Lower Red River Meadow Restoration Project, Idaho, U.S.A. *Restoration Ecology* 15:223–
750 239. <https://doi.org/10.1111/j.1526-100X.2007.00206.x>
- 751 Knowles, N., M.D. Dettinger, and D.R. Cayan, 2006. Trends in Snowfall versus Rainfall in the Western
752 United States. *Journal of Climate* 19:4545–4559. <https://doi.org/10.1175/JCLI3850.1>
- 753 Larkin, R.G. and J.M. Sharp, 1992. On the Relationship between River-Basin Geomorphology, Aquifer
754 Hydraulics, and Ground-Water Flow Direction in Alluvial Aquifers. *Geological Society of America*
755 *Bulletin* 104:1608–1620. [https://doi.org/10.1130/0016-
756 7606\(1992\)104%3C1608:OTRBRB%3E2.3.CO;2](https://doi.org/10.1130/0016-7606(1992)104%3C1608:OTRBRB%3E2.3.CO;2)
- 757 Lautz, L.K., 2008. Estimating Groundwater Evapotranspiration Rates Using Diurnal Water-Table
758 Fluctuations in a Semi-Arid Riparian Zone. *Hydrogeology Journal* 16:483–497.
759 <https://doi.org/10.1007/s10040-007-0239-0>
- 760 Lautz, L., C. Kelleher, P. Vidon, J. Coffman, C. Riginos, and H. Copeland, 2019. Restoring Stream
761 Ecosystem Function with Beaver Dam Analogues: Let’s Not Make the Same Mistake Twice.
762 *Hydrological Processes* 33:174–177. <https://doi.org/10.1002/hyp.13333>
- 763 Leake, S.A. and B. Gungle, 2012. Evaluation of Simulations to Understand Effects of Groundwater
764 Development and Artificial Recharge on Surface Water and Riparian Vegetation, Sierra Vista
765 Subwatershed, Upper San Pedro Basin, Arizona. U.S. Geological Survey Open-File Report 2012–
766 1206. <https://pubs.er.usgs.gov/publication/ofr20121206>

767 Leenhouts, J.M., J.C. Stromberg, R.L. Scott, S.J. Lite, M. Dixon, T. Rychener, E. Makings, D.G.
768 Williams, D.C. Goodrich, W.L. Cable, L.R. Levick, R. McGuire, R.M. Gazal, E.A. Yopez, P.
769 Ellsworth, and T.E. Huxman, 2006. Hydrologic Requirements of and Consumptive Ground-Water
770 Use by Riparian Vegetation along the San Pedro River, Arizona. U.S. Geological Survey Scientific
771 Investigations Report 2005-5163. <https://pubs.er.usgs.gov/publication/sir20055163>

772 McClain, M.E., Boyer, E.W., Dent, C.L., Gergel, S.E., Grimm, N.B., Groffman, P.M., Hart, S.C., Harvey,
773 J.W., Johnston, C.A., Mayorga, E. and McDowell, W.H., 2003. Biogeochemical hot spots and hot
774 moments at the interface of terrestrial and aquatic ecosystems. *Ecosystems*: 301-312.
775 <https://doi.org/10.1007/s10021-003-0161-9>

776 Macfarlane, W.W., J.M. Wheaton, N. Bouwes, M.L. Jensen, J.T. Gilbert, N. Hough-Snee, and J.A.
777 Shivik, 2017. Modeling the Capacity of Riverscapes to Support Beaver Dams. *Geomorphology*
778 *277*:72–99. <https://doi.org/10.1016/j.geomorph.2015.11.019>

779 Majerova, M., B.T. Neilson, N.M. Schmadel, J.M. Wheaton, and C.J. Snow, 2015. Impacts of Beaver
780 Dams on Hydrologic and Temperature Regimes in a Mountain Stream. *Hydrology and Earth*
781 *System Sciences* 19:3541–3556. <https://doi.org/10.5194/hess-19-3541-2015>

782 Malzone, J.M., C.S. Lowry, and A.S. Ward, 2016. Response of the Hyporheic Zone to Transient
783 Groundwater Fluctuations on the Annual and Storm Event Time Scales. *Water Resources Research*
784 *52*:5301–5321. <https://doi.org/10.1002/2015WR018056>

785 Nash, C.S., J.S. Selker, G.E. Grant, S.L. Lewis, and P. Noël, 2018. A Physical Framework for Evaluating
786 Net Effects of Wet Meadow Restoration on Late-Summer Streamflow. *Ecology* 11:1–15.
787 <https://doi.org/10.1002/eco.1953>

788 Nash, C.S., G.E. Grant, J.S. Selker, and S.M. Wondzell, 2020. Discussion: “Meadow Restoration
789 Increases Baseflow and Groundwater Storage in the Sierra Nevada Mountains of California” by
790 Luke J.H. Hunt, Julie Fair, and Maxwell Odland. *Journal of the American Water Resources*
791 *Association* 56:182–185. <https://doi.org/10.1111/1752-1688.12796>

792 Nash, C.S., G.E. Grant, S. Charnley, J.B. Dunham, H. Gosnell, M.B. Hausner, D.S. Pilliod, and J.D.
793 Taylor, 2021. Great Expectations: Deconstructing the Process Pathways Underlying Beaver-Related
794 Restoration. *BioScience* 71:249–267. <https://doi.org/10.1093/biosci/biaa165>

795 Naz, B.S., S.C. Kao, M. Ashfaq, H. Gao, D. Rastogi, and S. Gangrade, 2018. Effects of Climate Change
796 on Streamflow Extremes and Implications for Reservoir Inflow in the United States. *Journal of*
797 *Hydrology* 556:359–370. <https://doi.org/10.1016/j.jhydrol.2017.11.027>

798 Niswonger, R.G. and D.E. Prudic, 2005. Documentation of the Streamflow-Routing (SFR2) Package to
799 Include Unsaturated Flow beneath Streams - A Modification to SFR1. U.S. Geological Survey
800 Techniques and Methods 6-A13. <https://pubs.er.usgs.gov/publication/tm6A13>

801 Nyssen, J., J. Pontzele, and P. Billi, 2011. Effect of Beaver Dams on the Hydrology of Small Mountain
802 Streams: Example from the Chevral in the Ourthe Orientale Basin, Ardennes, Belgium. *Journal of*
803 *Hydrology* 402:92–102. <https://doi.org/10.1016/j.jhydrol.2011.03.008>

804 Persson, G., 1995. Willow Stand Evapotranspiration Simulated for Swedish Soils. *Agricultural Water*
805 *Management* 28:271–293. [https://doi.org/10.1016/0378-3774\(95\)01182-X](https://doi.org/10.1016/0378-3774(95)01182-X)

806 Pilliod, D.S., A.T. Rohde, S. Charnley, R.R. Davee, J.B. Dunham, H. Gosnell, G.E. Grant, M.B. Hausner,
807 J.L. Huntington, and C.S. Nash, 2018. Survey of Beaver-Related Restoration Practices in

808 Rangeland Streams of the Western USA. *Environmental Management* 61:58–68.
809 <https://doi.org/10.1007/s00267-017-0957-6>

810 Pollock, M.M., T.J. Beechie, and C.E. Jordan, 2007. Geomorphic Changes Upstream of Beaver Dams in
811 Bridge Creek, an Incised Stream Channel in the Interior Columbia River Basin, Eastern Oregon.
812 *Earth Surface Processes and Landforms* 32:1174–1185. <https://doi.org/10.1002/esp.1553>

813 Pollock, M.M., T.J. Beechie, J.M. Wheaton, C.E. Jordan, N. Bouwes, N. Weber, and C. Volk, 2014.
814 Using Beaver Dams to Restore Incised Stream Ecosystems. *BioScience* 64:279–290.
815 <https://doi.org/10.1093/biosci/biu036>

816 Pollock, M.M., G. Lewallen, K. Woodruff, C.E. Jordan, and J.M. Castro (Editors), 2018. The Beaver
817 Restoration Guidebook: Working with Beaver to Restore Streams, Wetlands, and Floodplains,
818 Version 2.01. United States Fish and Wildlife Service, Portland, Oregon.
819 <https://www.fws.gov/media/beaver-restoration-guidebook> [accessed 6/19/2022]

820 Prudic, D.E., 1989. Documentation of a Computer Program to Simulate Stream-Aquifer Relations Using
821 a Modular, Finite-Difference, Ground-Water Flow Model. U.S. Geological Survey Open-File
822 Report 88–729. <https://pubs.er.usgs.gov/publication/ofr88729>

823 Sawyer, A.H., M.B. Cardenas, A. Bomar, and M. Mackey, 2009. Impact of Dam Operations on
824 Hyporheic Exchange in the Riparian Zone of a Regulated River. *Hydrological Processes* 23:2129–
825 2137. <https://doi.org/10.1002/hyp.7324>

826 Scamardo, J. and E. Wohl, 2020. Sediment Storage and Shallow Groundwater Response to Beaver Dam
827 Analogues in the Colorado Front Range, USA. *River Research and Applications* 36:398–409.
828 <https://doi.org/10.1002/rra.3592>

829 Schmadel, N.M., A.S. Ward, C.S. Lowry, and J.M. Malzone, 2016. Hyporheic Exchange Controlled by
830 Dynamic Hydrologic Boundary Conditions. *Geophysical Research Letters* 43:4408–4417.
831 <https://doi.org/10.1002/2016GL068286>

832 Scott, R.L., E.A. Edwards, W.J. Shuttleworth, T.E. Huxman, C. Watts, and D.C. Goodrich, 2004.
833 Interannual and Seasonal Variation in Fluxes of Water and Carbon Dioxide from a Riparian
834 Woodland Ecosystem. *Agricultural and Forest Meteorology* 122:65–84.
835 <https://doi.org/10.1016/j.agrformet.2003.09.001>

836 Shah, N., M. Nachabe, and M. Ross, 2007. Extinction Depth and Evapotranspiration from Ground Water
837 under Selected Land Covers. *Ground Water* 45:329–338. [https://doi.org/10.1111/j.1745-
838 6584.2007.00302.x](https://doi.org/10.1111/j.1745-6584.2007.00302.x)

839 Shaw, G.D., M.H. Conklin, G.J. Nimz, and F. Liu, 2014. Groundwater and Surface Water Flow to the
840 Merced River, Yosemite Valley, California: ^{36}Cl and Cl^- Evidence. *Water Resources Research*
841 50:1943–1959. <https://doi.org/10.1002/2013WR014222>

842 Theis, C. V., 1940. The Source of Water Derived from Wells. *Civil Engineering* 10(5):277–280.

843 Ward, A.S., N.M. Schmadel, S.M. Wondzell, M.N. Gooseff, and K. Singha, 2017. Dynamic Hyporheic
844 and Riparian Flow Path Geometry through Base Flow Recession in Two Headwater Mountain
845 Stream Corridors. *Water Resources Research* 53:3988–4003.
846 <https://doi.org/10.1002/2016WR019875>

847 Ward, A.S. and A.I. Packman, 2019. Advancing Our Predictive Understanding of River Corridor
848 Exchange. *Wiley Interdisciplinary Reviews: Water* 6:e1327. <https://doi.org/10.1002/wat2.1327>

- 849 Weber, N., N. Bouwes, M.M. Pollock, C. Volk, J.M. Wheaton, G. Wathen, J. Wirtz, and C.E. Jordan,
850 2017. Alteration of Stream Temperature by Natural and Artificial Beaver Dams. PLoS ONE 12:1–
851 23. <https://doi.org/10.1371/journal.pone.0176313>
- 852 Wegener, P., T. Covino, and E. Wohl, 2017. Beaver-Mediated Lateral Hydrologic Connectivity, Fluvial
853 Carbon and Nutrient Flux, and Aquatic Ecosystem Metabolism. Water Resources Research
854 53:4606–4623. <https://doi.org/10.1002/2016WR019790>
- 855 Westbrook, C.J., D.J. Cooper, and B.W. Baker, 2006. Beaver Dams and Overbank Floods Influence
856 Groundwater-Surface Water Interactions of a Rocky Mountain Riparian Area. Water Resources
857 Research 42:1–12. <https://doi.org/10.1029/2005WR004560>
- 858 Winter, T.C., J.W. Harvey, O.L. Franke, and W.M. Alley, 1998. Groundwater and Surface Water a Single
859 Resource. U.S. Geological Survey Circular 1139. <https://pubs.er.usgs.gov/publication/cir1139>
- 860 Woessner, W.W., 2000. Stream and Fluvial Plain Ground Water Interactions: Rescaling Hydrogeologic
861 Thought. Groundwater 38:423–429. <https://doi.org/10.1111/j.1745-6584.2000.tb00228.x>
- 862 Wroblicky, G.J., M.E. Campana, H.M. Valett, and N. Dahm, 1998. Seasonal Variation in Surface-
863 Subsurface Water Exchange and Lateral Hyporheic Area of Two Stream-Aquifer Systems. Water
864 Resources Research 34:317–328. <https://doi.org/10.1029/97WR03285>
- 865

TABLES

867 TABLE 1. Summary of models used to explore various BMR designs in different hydrogeologic settings.

Design scenario	Hydrogeologic setting		
	Gaining Stream (G)	Losing Stream (L)	Strongly Losing Stream (SL)
Baseline (B)	G-B	L-B	SL-B
On-Channel Structure (S)	G-S	L-S	SL-S
Near Channel Activation (NC)	G-NC	L-NC	SL-NC
Far Channel Activation (FC)	G-FC	L-FC	SL-FC
Floodplain Inundation (FI)	G-FI	L-FI	SL-FI
Off-Channel Pond (OC)	G-OC	L-OC	SL-OC

TABLE 2. Summary of annual water budget results for model year 4.

Scenario	Change in Gross Stream Loss (m ³ yr ⁻¹)	Change in Gross Stream Gain (m ³ yr ⁻¹)	Change in Net Stream Gain (m ³ yr ⁻¹)	Change in Groundwater Outflow (m ³ yr ⁻¹)	Average Change in annual head amplitude (m yr ⁻¹)	Change in Dynamic Storage (m ³ yr ⁻¹)
G-S	20,285	19,122	-1,163	1,408	0.04	782
G-NC	19,923	18,551	-1,371	1,381	0.04	782
G-FC	20,396	18,851	-1,545	1,367	0.04	857
G-FI	20,168	18,834	-1,333	1,411	0.05	920
G-OC	8,869	4,714	-4,155	4,289	0.07	1,344
L-S	15,686	14,363	-1,324	1,357	-0.15	-3,070
L-NC	15,053	14,013	-1,040	1,386	-0.06	-1,159
L-FC	15,523	14,329	-1,194	1,375	-0.05	-1,096
L-FI	15,426	14,125	-1,301	1,385	-0.05	-998
L-OC	3,468	17	-3,451	3,711	0.14	2,713
SL-S	12,282	7,402	-4,880	3,711	0.00	-1
SL-NC	11,566	6,781	-4,785	3,659	0.00	-22
SL-FC	12,200	7,301	-4,899	3,714	0.00	45
SL-FI	12,042	7,112	-4,930	3,755	0.01	136
SL-OC	5,355	-135	-5,491	5,220	0.12	2,367

Table 3. Summary of results for mid-August of model year 4 (Stress Period 240).

Scenario	Change in Gross Stream Loss (m³ d⁻¹)	Change in Gross Stream Gain (m³ d⁻¹)	Change in Net Stream Gain (m³ d⁻¹)	Change in Groundwater Outflow (m³ d⁻¹)	Minimum Head Change (m)	Maximum Head Change (m)	Average Head Change (m)
G-S	55.2	60.7	5.5	4.9	0.01	0.18	0.08
G-NC	54.2	59.9	5.7	4.8	0.01	0.19	0.08
G-FC	54.9	60.8	5.8	4.9	0.01	0.18	0.08
G-FI	54.4	60.8	6.4	5.1	0.01	0.19	0.08
G-OC	19.3	31.3	11.9	16.0	0.10	0.78	0.55
L-S	42.2	48.0	5.9	4.8	0.01	0.18	0.07
L-NC	41.3	47.4	6.0	4.7	0.01	0.18	0.08
L-FC	41.8	48.0	6.2	4.8	0.01	0.18	0.08
L-FI	41.1	48.0	6.8	5.0	0.01	0.19	0.08
L-OC	5.7	18.3	12.6	14.8	0.03	0.50	0.25
SL-S	27.9	26.3	-1.6	9.5	0.02	0.19	0.09
SL-NC	21.4	20.1	-1.3	5.9	0.02	0.19	0.09
SL-FC	27.4	26.2	-1.2	9.6	0.02	0.19	0.09
SL-FI	26.6	25.8	-0.8	9.9	0.02	0.20	0.09
SL-OC	1.8	8.4	6.6	20.5	0.03	0.38	0.20

870

871

872 TABLE 4. Summary of sensitivity analysis (FC models). Response values are differences in weekly averages during
 873 mid-August of year 4. †

Hydrogeologic Setting	Change in Net Stream Gain (m ³ d ⁻¹)				
	0.025	0.25	2.5	25 [‡]	250
Hydraulic Conductivity (<i>K</i> ; m d ⁻¹)					
G	2.6	6.8	8.5	5.8	-14.8
L	2.6	6.8	8.8	6.2	-20.7
SL	2.6	7.0	8.7	-1.2	-31.5
Specific Yield (<i>S_y</i> ; unitless)	0.02	0.1	0.2 [‡]	0.3	0.4
G	-3.5	0.8	5.8	8.7	10.1
L	-3.7	0.9	6.2	9.1	10.7
SL	-8.4	-7.6	-1.2	3.5	6.8
Streambed Conductance (m ² d ⁻¹ m ⁻¹)	0.005	0.05	0.5 [‡]	5	50
G	-0.7	-1.6	5.8	1.7	0.1
L	-0.3	-1.6	6.2	1.6	-0.8
SL	-0.3	-3.2	-1.2	1.0	-1.1
Drain Conductance (m ² d ⁻¹)	0.1	1	10 [‡]	100	1000
G	10.3	8.7	5.8	5.0	4.8
L	10.3	8.9	6.2	5.1	5.1
SL	10.3	9.0	-1.2	-3.3	-3.4
Maximum ET Rate (<i>ET_{max}</i> ; mm yr ⁻¹)*	0 [‡]	150	300	600	1200
G	5.8	2.2	-1.4	-7.6	-25.0
L	6.2	2.4	-1.1	-10.1	-26.3
SL	-1.2	-6.6	-11.2	-17.1	-22.0
ET Extinction Depth (<i>ET_{XD}</i> ; m)*	0 [‡]	1	2	3	5
G	5.8	5.4	-7.6	-11.9	-10.1
L	6.2	6.2	-10.1	-14.0	-5.8
SL	-1.2	-1.2	-17.1	-9.2	-4.4

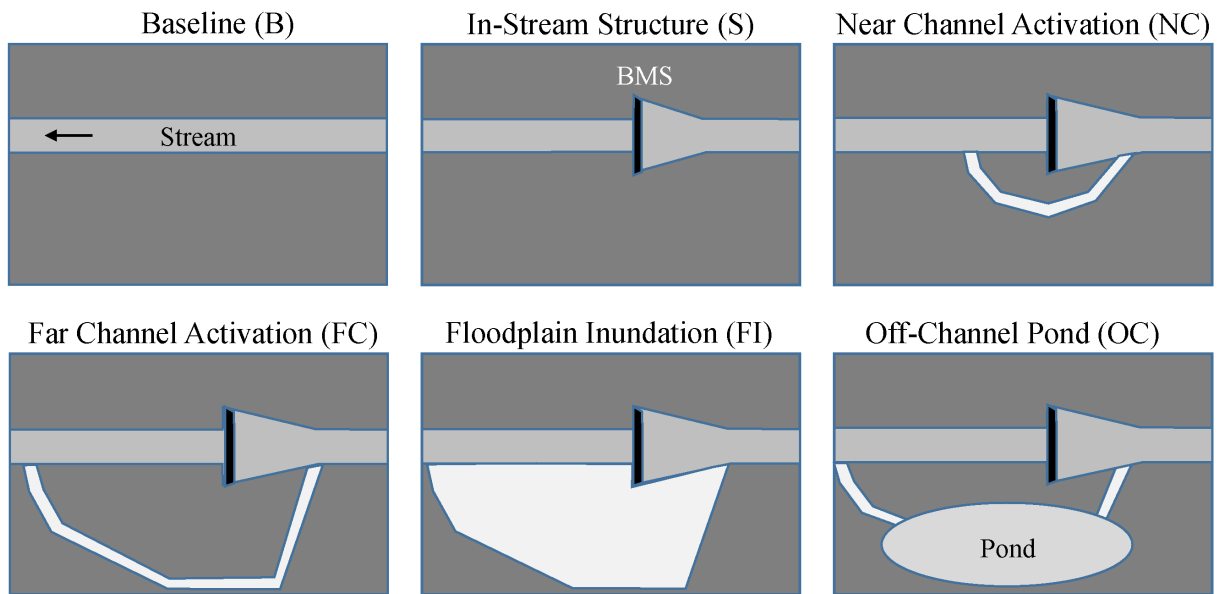
† The change in net stream gain is calculated as the difference between a baseline model with the parameter of interest at the value indicated, and the FC scenario with the parameter at the same value.

‡ indicates values used for scenario-testing

* for testing the effects of *ET_{max}* *ET_{XD}* was set to 2 m, and for testing *ET_{XD}* *ET_{max}* was set to 600 mm yr⁻¹.

875

FIGURES



876

877 FIGURE 1. Plan views of conceptual schematics for scenarios selected to explore common beaver-
878 mimicry stream restoration (BMR) treatment designs (also see table 1).

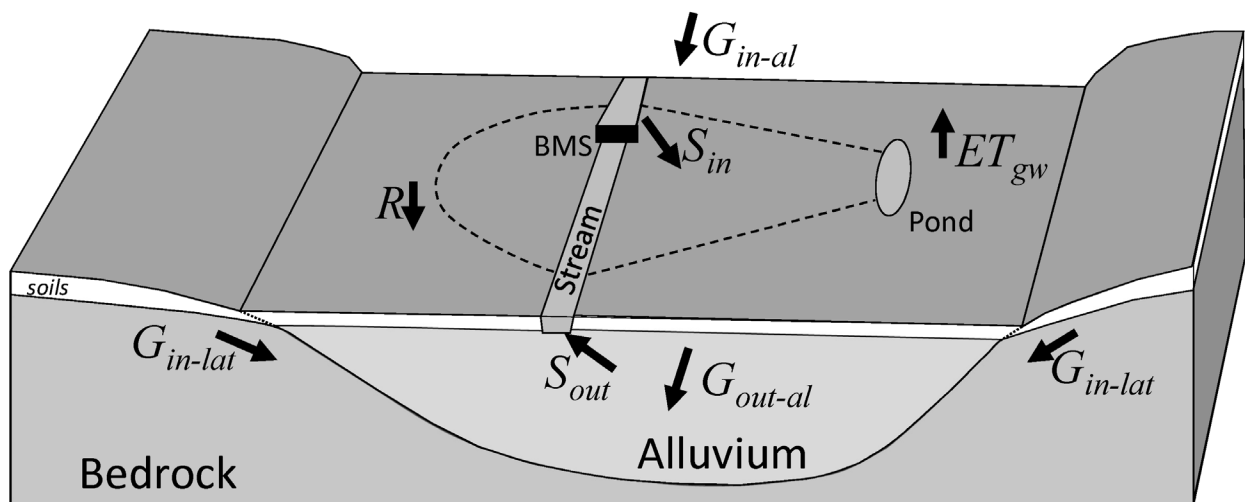
879

880

881

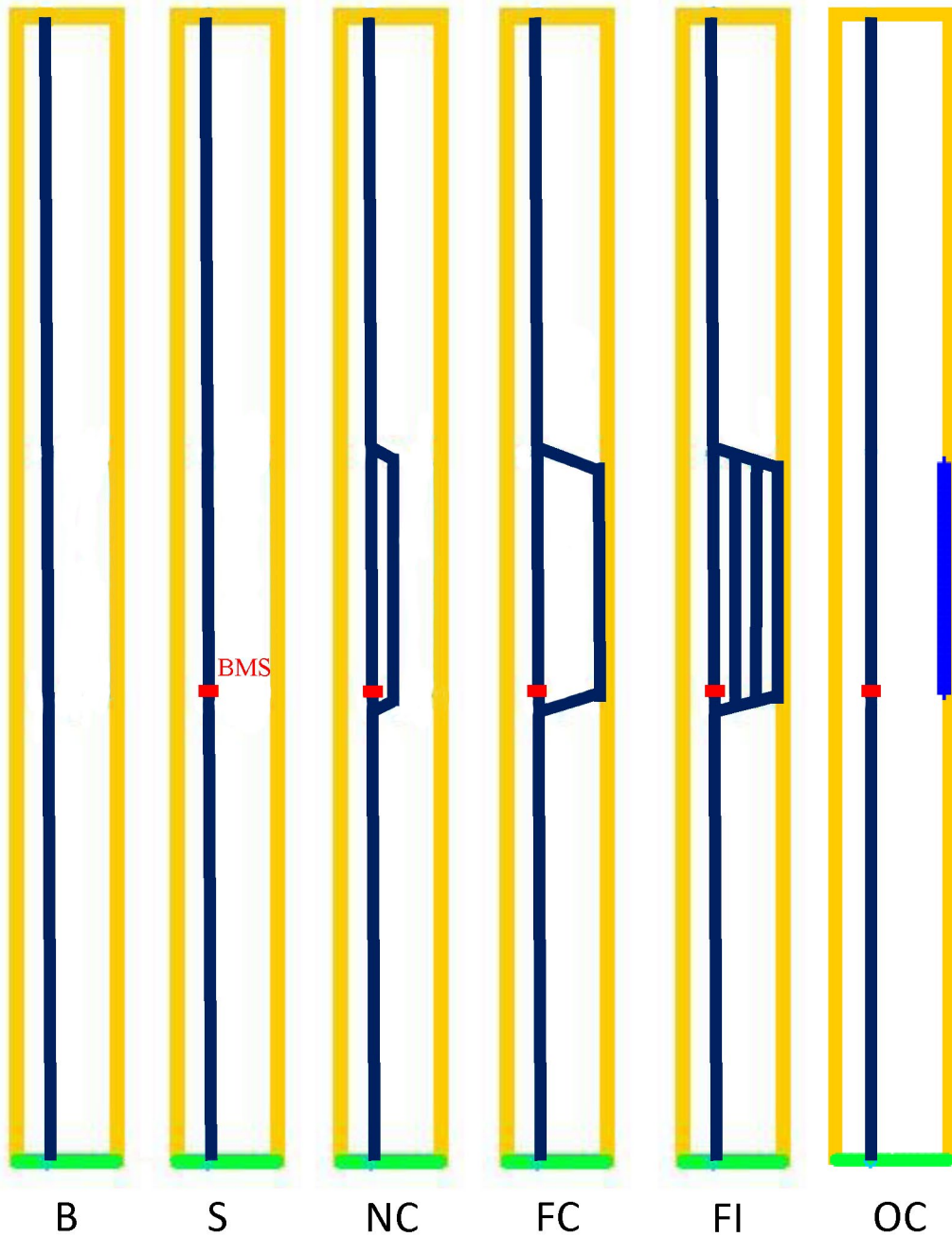
882

883



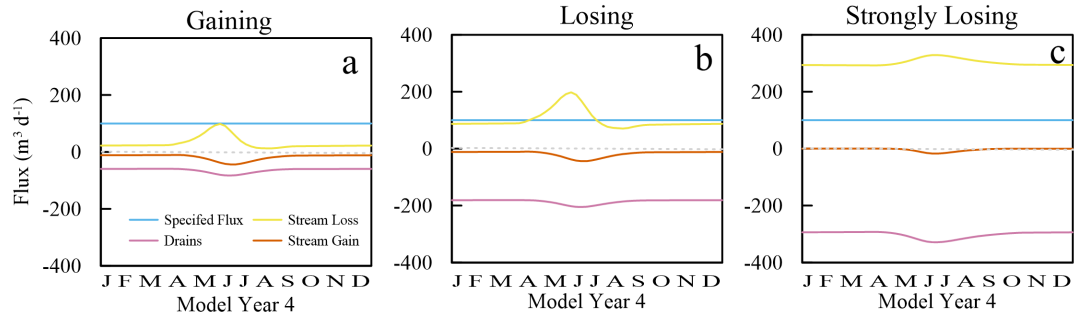
884

885 FIGURE 2. Conceptual block model of the stream/aquifer system used to design the simplified
886 groundwater modeling domains for the BMR model scenarios (see eqn. 1 for term definitions).



887

888 FIGURE 3. Plan view of the numerical models for each of the treatment types. The models had specified
 889 flux boundaries (yellow) along the upstream and lateral edges, drains (green) along the downstream
 890 edge, and stream boundaries on the cells adjacent to surface flow (dark blue). For the OC scenario the
 891 pond was simulated by adding a river boundary (bright blue) at the same location as the FC channel. The
 892 red boxes show the BMS locations. The main channel always had flow and side channels were active
 893 only during high flows in the NC, FC and FI scenarios.



894

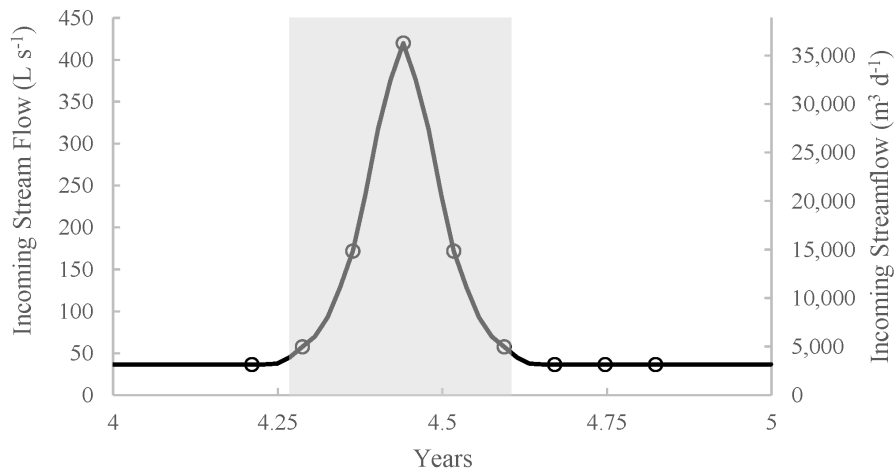
895 FIGURE 4. Flux values for the boundaries in the baseline models over the last year of simulations (model
 896 year 4). Positive values are inputs to the aquifer, and negative values are outputs from the aquifer.

897

898

899

900



901

902 FIGURE 5. The simplified snowmelt driven stream hydrograph used for model boundary conditions based
 903 on the stream package. The duration of diversion is shown in gray, as defined by the period when 10% of
 904 the streamflow was diverted in the NC, FC, and FI scenarios. The model output times shown with circles
 905 on this figure reflect the outputs shown for model year 4 on fig. 7a. Note that values are provided in both L
 906 s-1 and m3 d-1 to provide perspective for results from both the groundwater and surface-water
 907 perspectives.



908

909

910

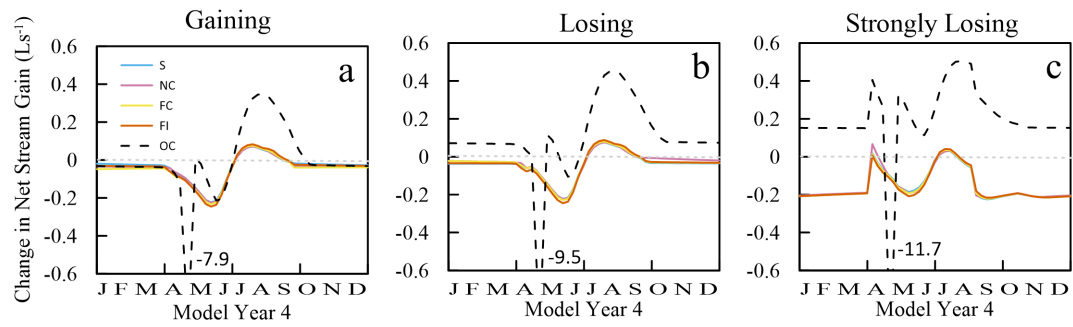
911

912

913

914

FIGURE 6. Top panels represent simulated gross stream gains (i.e. groundwater discharge to the stream) plotted vs. gross stream loss (i.e. groundwater recharge from the stream) within the model domain, based on (A) annual totals during model year 4 and (B) average values for a week in mid-August. Off-channel pond scenario results are highlighted. Bottom panels represent change in net stream gain resulting from restoration for all model scenarios and groundwater settings, based on (C) annual totals during model year 4 and (D) average values for a week in mid-August.

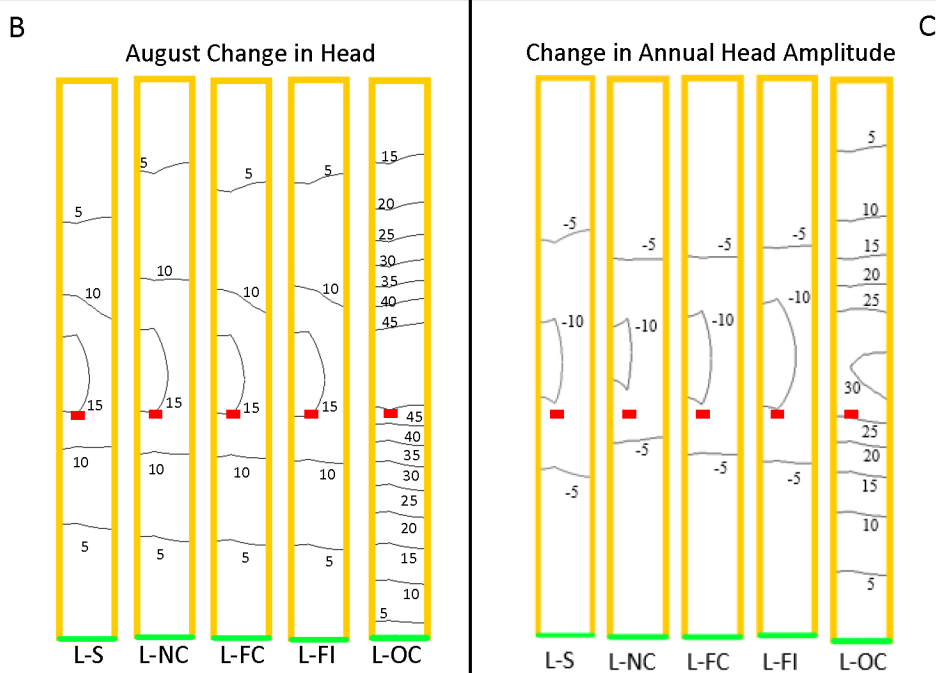
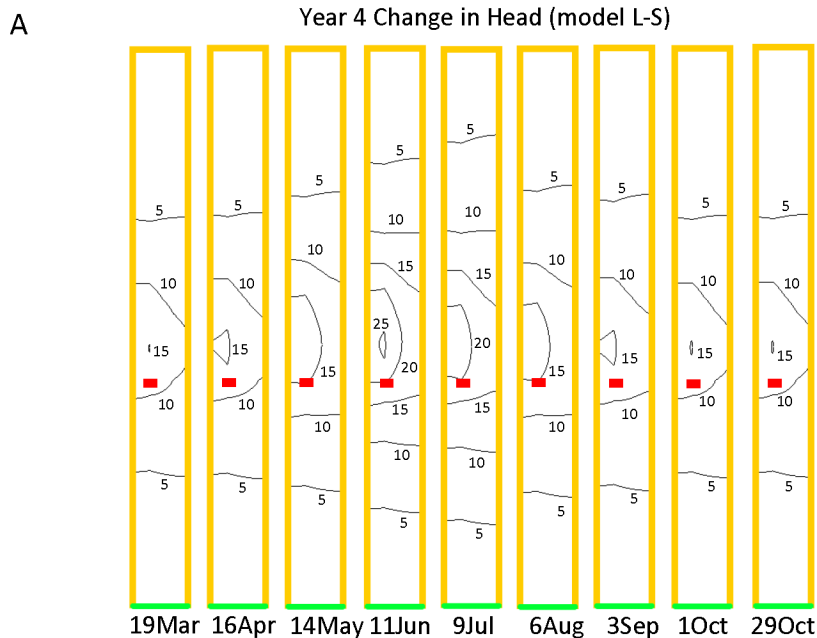


915

916

917

FIGURE 7. The change in net stream gains over model year 4 relative to the unrestored baseline simulation.



918

919 FIGURE 8. Examples of the changes in plan-view spatial head distribution created by BMS structures. (A)
 920 Seasonal dynamics in the amount the head was increased due to an BMS creating an on-channel pond in
 921 a losing hydrogeological context (S-L scenario). (B) Comparison of the amount that head was increased
 922 in mid-August across all BMS scenarios in the losing hydrogeological context. (C) The change in the
 923 seasonal amplitude of mounding compared across all BMS scenarios in the losing hydrogeological
 924 context. Red squares denote the location of the BMS and contour labels are in units of cm.

925

926

927

928
929
930
931
932
933
934
935
936
937
938
939
940
941
942
943
944
945
946

SUPPORTING INFORMATION

S1. Numerical Groundwater Modeling Details

S1.1 Baseline Models

Numerical groundwater flow models were developed using MODFLOW-2000 (Harbaugh et al., 2000), using the Groundwater Modeling System (GMS) version 9.2 user interface (Aquaveo, 2013). The Layer Property Flow (LPF) package, and the Preconditioned Conjugate Gradient (PCG2) solver were employed to solve the groundwater flow equations under transient conditions (Harbaugh et al., 2000). GMS software is currently available for free download at <https://www.aquaveo.com/downloads?tab=1#TabbedPanels>, which allows models to be viewed, but not modified. A GMS license is needed for model modification.

The three baseline models and the 15 models for the treatment scenarios (table 1 of the main text) are publicly available through the HydroShare database (<https://www.hydroshare.org/>). The reference is:

Bobst, A. L., R. Payn, G. Shaw (2021). GMS MODFLOW Simulations of Beaver-Mimicry Stream Restoration, HydroShare, <http://www.hydroshare.org/resource/d3b23a5e59cb408c8953b6eff2ee7b73>

The models were constructed to represent an aquifer 1,000 m long, 100 m wide, and 10 m thick (table S1.1 and fig. S1.1). The aquifer was spatially discretized using a single layer, with cells that were 2 m by 2 m in plan area (model domain of 500 cells long by 50 cells wide). The top and bottom of cells were defined by uniform planes with a drop of 5 m in elevation over the

Table S1.1. Details for Baseline Models

Spatial Units	m
Temporal Units	d
Reference Elevation	0 m
Maximum Elevation	15 m
Rows	500
Columns	50
Layers	1
Active Cells	25,000
Row Spacing	2 m
Column Spacing	2 m
Layer Thickness	10 m
Total Area	0.1 km ²
Slope of the Model Base	0.005
Stress Periods	261
Stress Period Duration ⁺	7 d
Time Steps Per Stress Period ⁺	7
Hydraulic Conductivity (K)	25 m d ⁻¹
Specific Yield (S _y)	0.2
Specific Storage (S _s)	0.0001 m ⁻¹
Specified Flux Cells (alluvium; WEL)	48
Specified Flux Cells (lateral; WEL)	998
DRN Cells	50
Drain Conductance	10 m ² d ⁻¹
Drain Elevation*	9, 7.5, or 4 m
STR Cells	895
Streambed Conductance	0.5 (m ² d ⁻¹) m ⁻¹

⁺The first stress period was run to steady-state, and had one, one-day time step. The last stress period had 8 1-day time steps.

*Different drain elevations were used for the gaining, losing and strongly losing simulations.



948

949 Figure S1.1. Map view of the model domain. The model domain is 100 m wide by 1,000 m long to
950 represent an alluvial valley aquifer. Specified Flux boundaries (WEL package; yellow) were used to
951 supply alluvial groundwater inflow at the upper end of the model domain, and lateral groundwater inflow
952 along the sides. The Drain package (DRN; green) was used at the lower end of the model to allow
953 groundwater to flow out of the model domain. The stream package (STR; blue) was used to simulate the
954 bidirectional exchange of water between the aquifer and the stream. For the baseline model simulations,
955 no water was diverted from the main stem into the side channels.

956

957 1,000 m length of the model domain (valley gradient of 0.005). A single layer of cells was used
958 because the effects to the water budget over a seasonal time scale was the output of greatest
959 interest, and the models were not intended to evaluate changes in vertical gradients or the details
960 of flow lines adjacent to the structures.

961 The models simulated transient hydrologic conditions over time and were run for 5 years
962 (1,826 days), using 261 stress periods. The first stress period was run to steady-state so that the
963 model used a long-term equilibrium state to define initial conditions for the subsequent time-
964 dependent stress periods. All stress periods had 7 1-day time steps, except for the first (1 day,
965 steady-state), and the last (8 1-day time steps).

966 Aquifer properties were homogeneous and isotropic throughout the model domain and
967 were based on literature values for a coarse sand aquifer. K was set to 25 m d^{-1} , specific yield (S_y)
968 was 0.2, and specific storage (S_s , which has little influence on an unconfined model) was 1×10^{-4}
969 m^{-1} (Fetter, 1994; Freeze and Cherry, 1979; Heath, 1983).

970 Specified flux boundaries were defined on the upstream and lateral edges of the model
971 domain (fig. S1.1) using the WEL package. The bottom of the model domain was a no-flow
972 boundary. The upstream edge of the model represented groundwater inflow through the
973 alluvium, which was defined at a constant rate of $95 \text{ m}^3 \text{ d}^{-1}$ distributed evenly over the boundary.
974 The lateral edges of the model represented groundwater inflow from the adjacent hillslopes and
975 bedrock, which was defined at a constant rate of $5 \text{ m}^3 \text{ d}^{-1}$ distributed evenly over both of the
976 lateral boundaries.

977 At the downstream end of the model domain, groundwater outflow was simulated using
978 the drain package (DRN; fig. S1.1) (Banta, 2000). The drain conductance was set to $10 \text{ m}^2 \text{ d}^{-1}$,
979 which provided for adequate groundwater outflow, and did not create flooding. The elevations of

980 the drains were used to control the groundwater levels within the model domain, and thus
981 develop models of stream reaches that were generally gaining, losing, or strongly losing (Winter
982 et al., 1998) (table S1.1). Drains were set at an elevation 1 m below the floodplain surface to
983 create gaining streams, 2.5 m below the floodplain surface to create losing streams, and 6 m
984 below the floodplain surface to create strongly losing streams.

985 The STR stream package (Prudic, 1989) was used to simulate the exchange of water
986 between the stream channels and the alluvial aquifer (fig. S1.1). The stream elements were
987 straight (sinuosity = 1) and the main stem was set 31 m from the left edge of the model domain
988 (fig. S1.1; column 16). The channel was simulated to be 1 m wide with a rectangular cross
989 section. Manning's roughness coefficient was set at 0.05 to be similar to values reported for
990 mountain streams (Barnes, 1969), and representing the roughness of the riffles which form the
991 control structures. The top of the streambed was set 1 m below the floodplain surface. The
992 equation for calculating streambed conductance for a unit length of stream bed is (Prudic, 1989):

$$993 \quad C_{str} = (K_{bed}W)/M$$

994 where C_{str} is the streambed conductance, K_{bed} is the vertical hydraulic conductivity of the
995 streambed sediments, W is the width of the streambed, and M is the thickness of the streambed
996 sediments. Streambed conductance was calculated based on the vertical hydraulic conductivity of
997 a stream with a silt bottom (0.5 m d^{-1}), similar to the sediments in the pools, which tend to
998 dominate the pool-riffle streams that we work with. The streambed sediments were set to 1 m
999 thick over a 1 m wide streambed, resulting in a conductance per unit length of stream of 0.5 m^2
1000 $\text{d}^{-1} \text{ m}^{-1}$.

1001 The annual streamflow hydrograph for flow into the upstream end of the main stem was
1002 based on a simplified symmetrical snowmelt driven stream hydrograph (see fig. 5 in the main

1003 text), with an average streamflow of 100 L s^{-1} , peak flows of 420 L s^{-1} , and baseflows of 37 L s^{-1} .

1004 An identical hydrograph was used for each year simulated.

1005 Effects of ET_{gw} and groundwater recharge from local precipitation were not included in
1006 the baseline models to allow for unconfounded comparisons of the fundamental behavior of
1007 groundwater storage among those scenarios which results from different types of BMR
1008 treatments in different hydrogeologic settings. ET_{gw} was simulated for the sensitivity analysis
1009 (see supporting information section S2.1).

1010

1011 **S1.2 Scenarios**

1012 **On-Channel Structure (S).** The effects of an on-channel structure were simulated by
1013 introducing a step in the slope of the streambed relative to the baseline configuration. The
1014 upstream portion of the step had a relatively shallow slope (gradient of 0.0002) to represent the
1015 pool behind the BMS. At the BMS the streambed steeply dropped across one cell to the level of
1016 the baseline (a 1 m drop over 2 m). This caused the streambed to be at an elevation 1 m higher
1017 than the baseline at the location of the BMS. As with the baseline simulations, all surface flow
1018 was directed through the main stem of the stream channel. All other treatment scenarios include
1019 this structure and its effects, with added variations including seasonal activation of side channels,
1020 floodplain inundation, or creation of an off-channel pond in the adjacent floodplain. While this
1021 approach allows for simulation of effects to the groundwater system due to changes in stream
1022 stage, it does not explicitly simulate the effects of surface water storage from the pond. As such,
1023 our analysis only addresses the groundwater-mediated effects of BMR.

1024 **Side-Channel Activation and Floodplain Inundation (NC, FC, and FI).** Additional
1025 stream channels were defined to include the effects of the activation of secondary channels or
1026 floodplain inundation along with the effects of the on-channel pool created by the BMS.
1027 Individual channels were activated for the “near channel” (NC) and “far channel” (FC) scenarios,
1028 which simulate the influence of individual activated channels proximal to, or distal from, the
1029 main channel. STR parameters for the secondary channels were set to the same values as those of
1030 the main stem. The simulated secondary channel for NC scenarios was 22 m away from the main
1031 stem, and the simulated secondary channel for FC scenarios was 64 m from the main stem (fig.
1032 S1.1). Floodplain inundation (FI) scenarios were simulated by using both the NC and FC
1033 channels, plus an additional channel half way between them (43 m from the main stem). Again,

1034 all STR parameters were the same as the main stem. The NC, FC, and FI scenarios were all
1035 configured to activate the secondary channels during high flow conditions. The stream baseflow
1036 was 37 L s^{-1} , and when flow was greater than 40 L s^{-1} , 10% of the flow was diverted into either
1037 the near channel (NC), the far channel (FC), or split evenly among the three side channels (FI).
1038 This configuration resulted in side channel activation for 19 weeks each year, from mid-April to
1039 early-August.

1040 **Off-Channel Pond (OC).** MODFLOW's river package (Harbaugh et al., 2000) was used
1041 to simulate the creation of an off-channel pond in addition to the on-channel pool created by the
1042 BMS. We conceptualized the pond as a floodplain depression that is filled during high flows by a
1043 secondary channel activated by a BMS. The stage in the pond was subsequently conceptualized
1044 to decrease throughout the summer, at rates reasonable for the pond outputs of infiltration and
1045 evaporation, given a pond approximately 30 m wide, 200 m long, and with 600 mm/yr of
1046 evaporation. The pond was placed in the same location as the FC secondary channel; 64 m from
1047 the main stem (fig. S1.1). The conductance of the river boundary was set to zero during the time
1048 when the pond would be dry, to ensure that the boundary provided no recharge when it would be
1049 dry from fall to early spring. The riverbed conductance was set the same as the main stem of the
1050 stream while it was wet. The stage at the downstream end of the pond was set at the land surface
1051 in late-April to represent pond filling during snowmelt. The stage at the upstream end of the
1052 pond was set 1 m below land surface so that the pond surface was flat. The stage at the
1053 downstream end was configured to decrease linearly to 1 m below land surface in mid-
1054 September, providing recharge to the aquifer for a period of 21 weeks. This caused the surface
1055 area over which recharge is occurring to remain constant, while the head changes.

1056 **S1.3 Model Limitations and Assumptions**

1057 There are several limitations and assumptions that are inherent in using a single layer
1058 MODFLOW 2000 model with the Layer-Property Flow (LPF) package to simulate groundwater flow in
1059 an unconfined aquifer, and the bidirectional movement of water between surface waters and the aquifer
1060 (Anderson et al., 2015; Brunner et al., 2010; Harbaugh et al., 2000). These include 1) the groundwater
1061 flow equation is applicable; 2) changes in saturated thickness, and therefore changes in transmissivity (T),
1062 are negligible at the timestep time scale; 3) effects of unsaturated flow are negligible; and 4) vertical
1063 gradients are small, so that using a single layer does not result in large errors in simulating the height of
1064 groundwater mounds.

1065 MODFLOW 2000 uses the groundwater flow equation as its governing equation for routing
1066 groundwater through the model domain. This based on Darcy's Law and mass balance (Anderson et al.,
1067 2015; Harbaugh et al., 2000; McDonald and Harbaugh, 1988). It assumes that there is a single-phase fluid
1068 at a constant density moving through a continuous porous medium. Darcy's Law is not valid when there
1069 is turbulent flow through the sediments. These assumptions are valid for our conceptual model.

1070 The horizontal hydraulic conductance between two cells in MODFLOW 2000 is based on the T
1071 of the two cells and the cell geometry (Harbaugh et al., 2000). A cell's T value is the product of its
1072 hydraulic conductivity (K) and the saturated thickness of the cell. For an unconfined aquifer the saturated
1073 thickness will change over time as head changes. Convertible cells were used to represent the unconfined
1074 aquifer in our models, and for convertible cells T values are recalculated at the start of each iteration,
1075 using the saturated thickness resulting from the preceding iteration (Harbaugh et al., 2000). Since we used
1076 relatively short (one day) timesteps, errors introduced by variations in T should be small.

1077 The stream package (STR) assumes that streams are directly connected to the aquifer, and that
1078 any effects of the water passing through the unsaturated zone are negligible. Due to this limitation
1079 disconnected losing streams (Winter et al., 1998) can not be simulated (although they can be simulated
1080 using MODFLOW's SFR package). The errors due to this approximation should be small since for our

1081 models the depth to groundwater was only a few meters and the recharge occurs over several months
1082 (Niswonger and Prudic, 2005).

1083 Using a single layer precludes simulation of vertical groundwater movement. If vertical gradients
1084 are important this can result in errors in simulated groundwater mounds (Brunner et al., 2010). For our
1085 conceptual model where a relatively permeable unconsolidated aquifer is underlain by low permeability
1086 bedrock, vertical groundwater movement is expected to be minor.

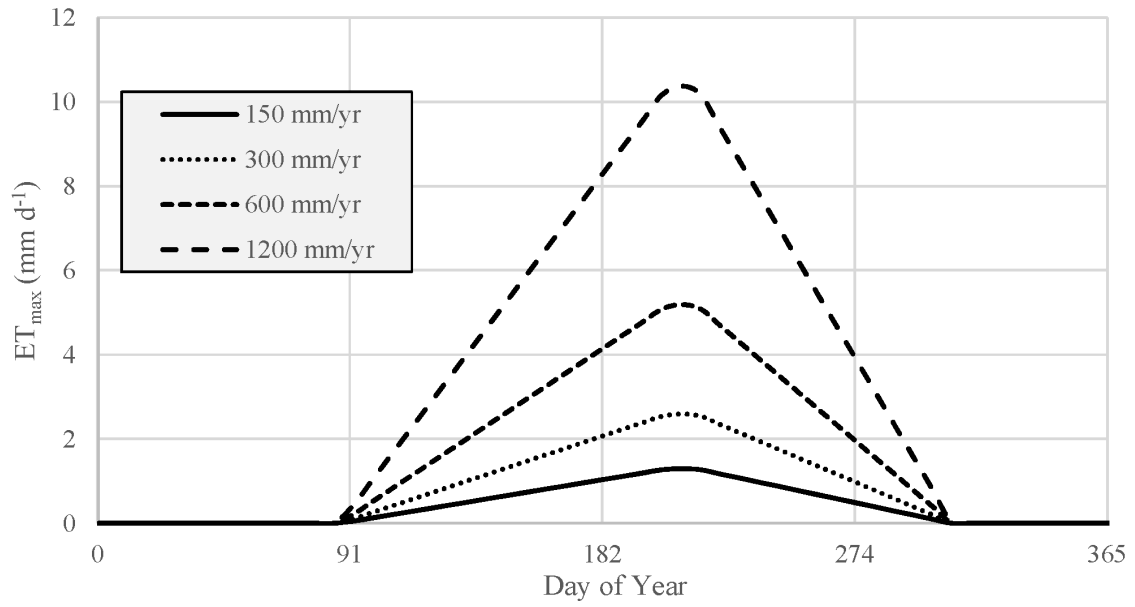
1087 *S2. Sensitivity Analysis*

1088 We conducted a sensitivity analysis to evaluate which parameters have the greatest
1089 influence on the outputs of interest. The primary output of interest was the change in dry-season
1090 net stream gains within the modeled reach due to the far channel (FC) BMR treatment. This
1091 treatment was selected for the sensitivity analysis because it showed effects near the middle of
1092 the range for the treatments that did not include an off-channel pond (OC), and so was
1093 considered to be representative to BMR treatments in general. This first-order sensitivity analysis
1094 included assessing the effects of different values of horizontal hydraulic conductivity (K_h),
1095 specific yield (S_y), streambed conductance, drain conductance, potential evapotranspiration
1096 (ET_{max}), and evapotranspiration extinction depth (ET_{XD}). This first-order approach only provides
1097 information about the independent influence of the parameter tested, not the interactions between
1098 parameters, since only one parameter was varied at a time. Global sensitivity analysis, including
1099 evaluating the interactions between parameters, would be an interesting avenue for future
1100 research. The range of parameters tested in this effort encompassed a wide range of plausible
1101 values for these settings. For instance, the K_h values tested would be appropriate for sediments
1102 ranging from silt to gravel (Heath, 1983).

1103 **S2.1 Model modifications**

1104 Groundwater evapotranspiration (ET_{gw}) was not included in the baseline models, or
1105 scenarios, but it was added for the sensitivity analysis. ET_{gw} was implemented in the models
1106 using MODFLOW's EVT package (McDonald and Harbaugh, 1988). In our model the ET_{gw} rate
1107 was assumed to be equal to potential ET (ET_{max}) when the simulated groundwater surface was at
1108 or above the land surface, and was negligible when the water table was below the extinction
1109 depth (ET_{XD}). When simulated groundwater levels are between the ET_{XD} and the land surface
1110 ET_{gw} rates vary linearly with depth between zero and ET_{max} .

1111 ET_{gw} was simulated for the entire model domain, and was simulated assuming ET_{max} is
1112 transient and correlated with seasonal air temperature variations typical to the northern Rocky
1113 Mountains of the United States (ET_{max} is zero in the winter, and the highest in late-July; fig.
1114 S2.1). The range of ET_{max} values tested ranged from zero to 1,200 mm yr⁻¹, representing rates
1115 appropriate for bare ground to dense willow stands. ET_{XD} values depend on plant and soil types,
1116 and the selected values (1 to 5 m) represent a range typical from grasses to trees and from silty
1117 clay loam to sand (Shah et al., 2007). For testing the effects of varying ET_{max} ET_{XD} was set to 2
1118 m, and for testing ET_{XD} ET_{max} was set to 600 mm yr⁻¹.



1119

1120 Figure S2.1. Transient potential ET rates (ET_{max}) were set to vary with air temperature.

1121

S2.2 Net Stream Gains

TABLE S2.1. Sensitivity Analysis

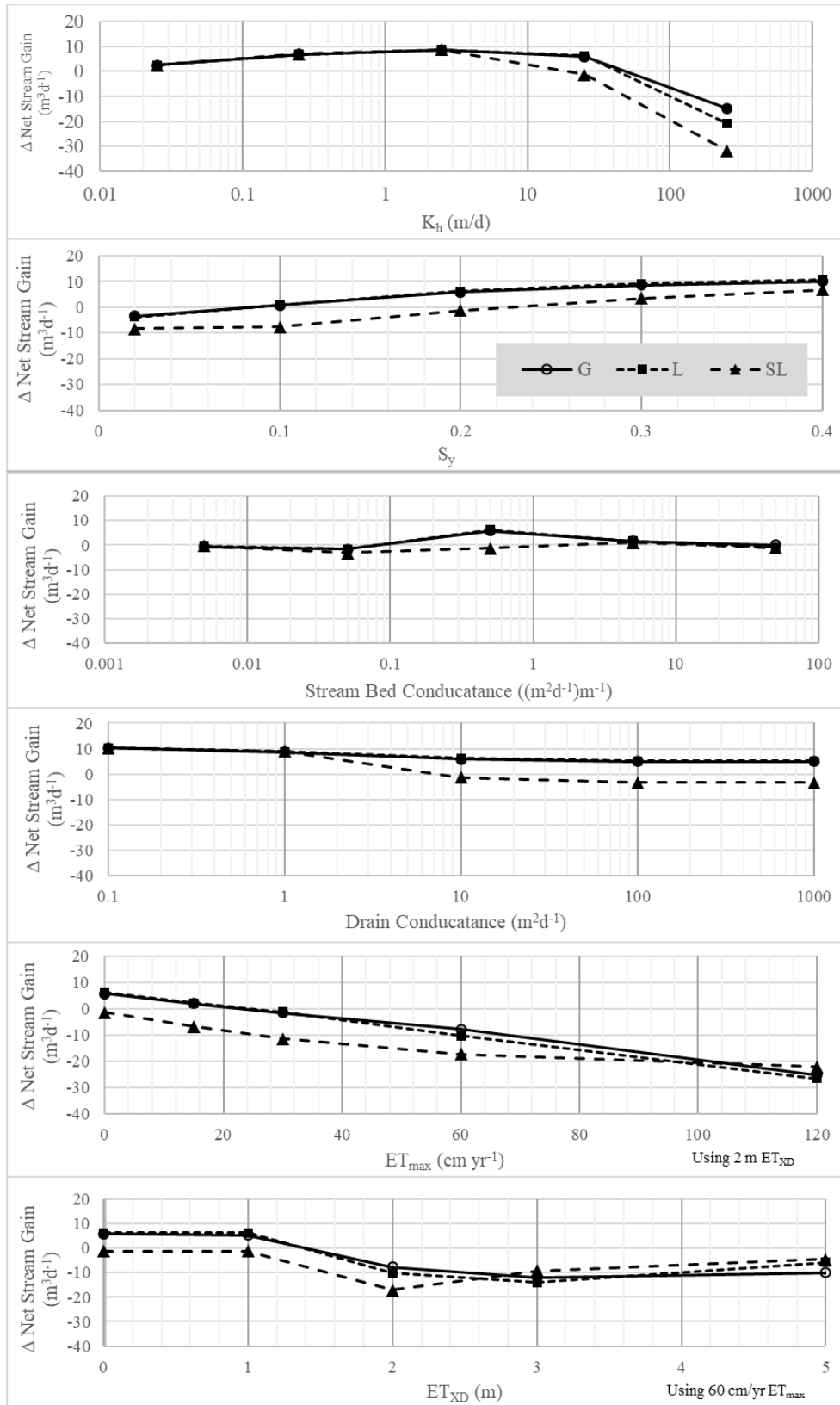
Change in Net Stream Gain due to FC BMR Treatment; Mid-August, Year 4 (m^3d^{-1})[†]

K_h (md^{-1})	0.025	0.25	2.5	25 [‡]	250
G	2.6	6.8	8.5	5.8	-14.8
L	2.6	6.8	8.8	6.2	-20.7
SL	2.6	7.0	8.7	-1.2	-31.5
S_v	0.02	0.1	0.2 [‡]	0.3	0.4
G	-3.5	0.8	5.8	8.7	10.1
L	-3.7	0.9	6.2	9.1	10.7
SL	-8.4	-7.6	-1.2	3.5	6.8
Streambed Conductance ($(\text{m}^2\text{d}^{-1})\text{m}^{-1}$)	0.01	0.1	0.5 [‡]	5	50
G	-0.7	-1.6	5.8	1.7	0.1
L	-0.3	-1.6	6.2	1.6	-0.8
SL	-0.3	-3.2	-1.2	1.0	-1.1
Drain Conductance (md^{-1})	0.1	1.0	10 [‡]	100	1000
G	10.3	8.7	5.8	5.0	4.8
L	10.3	8.9	6.2	5.1	5.1
SL	10.3	9.0	-1.2	-3.3	-3.4
ET_{max} (mm yr^{-1}) [*]	0 [‡]	150	300	600	1200
G	5.8	2.2	-1.4	-7.6	-25.0
L	6.2	2.4	-1.1	-10.1	-26.3
SL	-1.2	-6.6	-11.2	-17.1	-22.0
ET_{XD} (m) [*]	0 [‡]	1	2	3	5
G	5.8	5.4	-7.6	-11.9	-10.1
L	6.2	6.2	-10.1	-14.0	-5.8
SL	-1.2	-1.2	-17.1	-9.2	-4.4

[†] The change in net stream gain is calculated as the difference between a baseline model with the parameter at the value indicated, and a FC scenario with the parameter at the same value.

[‡] indicates values used for scenario testing models.

^{*} for testing the effects of ET_{max} ET_{XD} was set to 2 m, and for testing ET_{XD} ET_{max} was set to 600 mm yr^{-1} .



1123

1124 FIGURE S2.2. Changes in Net Stream Gain caused by implementing the FC scenario with different
 1125 model parameters.

S2.3 Gross Stream Loss

TABLE S2.2. Sensitivity Analysis

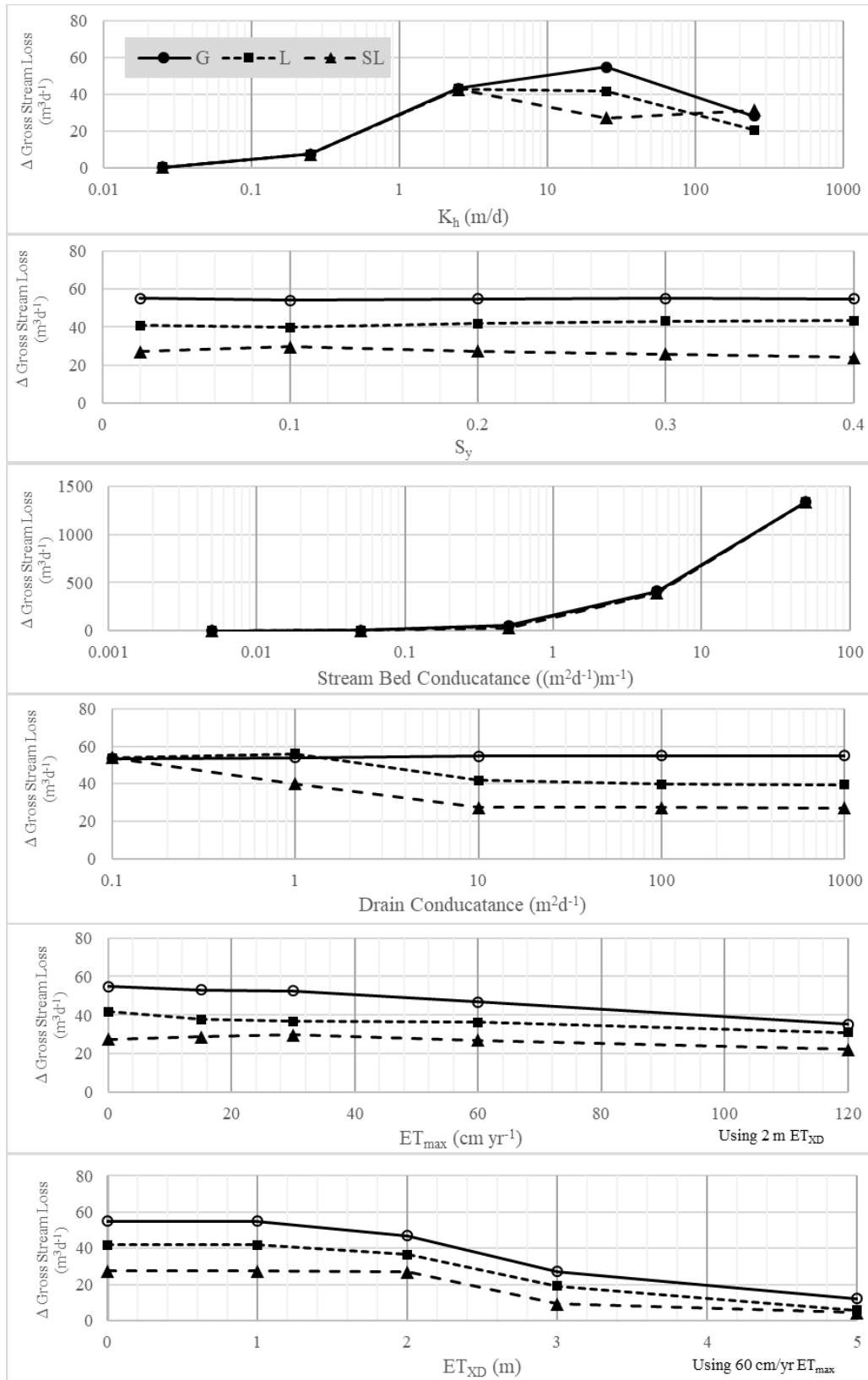
Change in Gross Stream Loss due to FC BMR Treatment; Mid-August, Year 4 (m^3d^{-1})[†]

K_h (md^{-1})	0.025	0.25	2.5	25 [‡]	250.0
G	0.4	7.7	43.4	54.9	28.5
L	0.4	7.7	43.3	41.8	20.7
SL	0.4	7.7	42.9	27.4	31.5
S_v	0.02	0.1	0.2 [‡]	0.3	0.4
G	54.9	54.1	54.9	55.1	54.7
L	40.7	39.8	41.8	43.1	43.3
SL	27.1	29.6	27.4	25.8	24.0
Streambed Conductance ($(\text{m}^2\text{d}^{-1})\text{m}^{-1}$)	0.01	0.1	0.5 [‡]	5	50
G	0.6	4.8	54.9	411.5	1338.0
L	0.3	1.6	41.8	401.1	1338.0
SL	0.3	3.2	27.4	387.9	1335.8
Drain Conductance (md^{-1})	0.1	1.0	10 [‡]	100	1000
G	53.5	54.2	54.9	55.0	55.0
L	53.7	56.1	41.8	39.7	39.4
SL	54.1	39.9	27.4	27.2	27.2
ET_{max} (mm yr^{-1}) [*]	0 [‡]	150	300	600	1200
G	54.9	53.0	52.5	46.8	35.3
L	41.8	37.9	36.8	36.4	31.0
SL	27.4	28.8	29.8	27.0	22.2
ET_{XD} (m) [*]	0 [‡]	1	2	3	5
G	54.9	54.9	46.8	27.1	12.2
L	41.8	41.8	36.4	19.0	5.8
SL	27.4	27.4	27.0	9.2	4.4

[†] The change in net stream gain is calculated as the difference between a baseline model with the parameter at the value indicated, and a FC scenario with the parameter at the same value.

[‡] indicates values used for scenario testing models.

^{*} for testing the effects of ET_{max} ET_{XD} was set to 2 m, and for testing ET_{XD} ET_{max} was set to 600 mm yr^{-1} .



1127

1128 FIGURE S2.3. Changes in Gross Stream Loss caused by implementing the FC scenario with different
 1129 model parameters. Note the different y-scale on the chart for streambed conductance.

S2.4 Gross Stream Gain

Table S2.3. Sensitivity Analysis

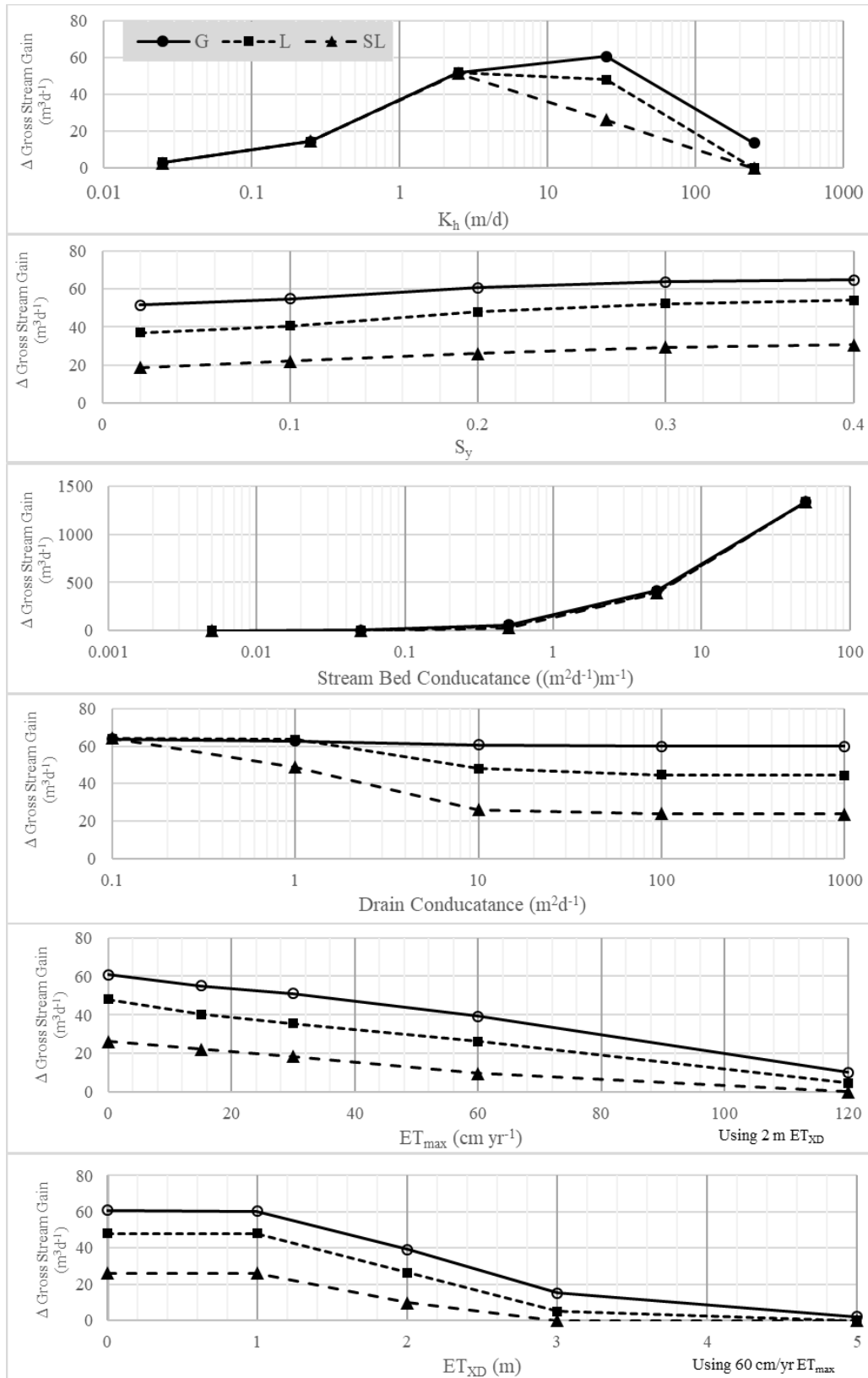
Change in Gross Stream Gain due to FC BMR Treatment; Mid-August, Year 4 (m^3d^{-1})[†]

K_h (md^{-1})	0.025	0.25	2.5	25 [‡]	250.0
G	3.0	14.4	51.9	60.8	13.7
L	3.0	14.5	52.0	48.0	0.0
SL	3.0	14.7	51.5	26.2	0.0
S_v	0.02	0.1	0.2 [‡]	0.3	0.4
G	51.4	54.9	60.8	63.7	64.8
L	37.0	40.7	48.0	52.2	54.0
SL	18.7	22.0	26.2	29.3	30.7
Streambed Conductance ($(\text{m}^2\text{d}^{-1})\text{m}^{-1}$)	0.01	0.1	0.5 [‡]	5	50
G	-0.1	3.2	60.8	413.2	1338.0
L	0.0	0.0	48.0	402.7	1337.2
SL	0.0	0.0	26.2	388.9	1334.7
Drain Conductance (md^{-1})	0.1	1.0	10 [‡]	100	1000
G	63.8	62.8	60.8	60.0	59.9
L	64.0	63.7	48.0	44.8	44.5
SL	64.4	48.9	26.2	24.0	23.8
ET_{max} (mm yr^{-1}) [*]	0 [‡]	150	300	600	1200
G	60.8	55.2	51.2	39.2	10.3
L	48.0	40.3	35.7	26.2	4.7
SL	26.2	22.2	18.5	9.9	0.3
ET_{XD} (m) [*]	0 [‡]	1	2	3	5
G	60.8	60.3	39.2	15.2	2.2
L	48.0	48.0	26.2	5.0	0.0
SL	26.2	26.2	9.9	0.0	0.0

[†] The change in net stream gain is calculated as the difference between a baseline model with the parameter at the value indicated, and a FC scenario with the parameter at the same value.

[‡] indicates values used for scenario testing models.

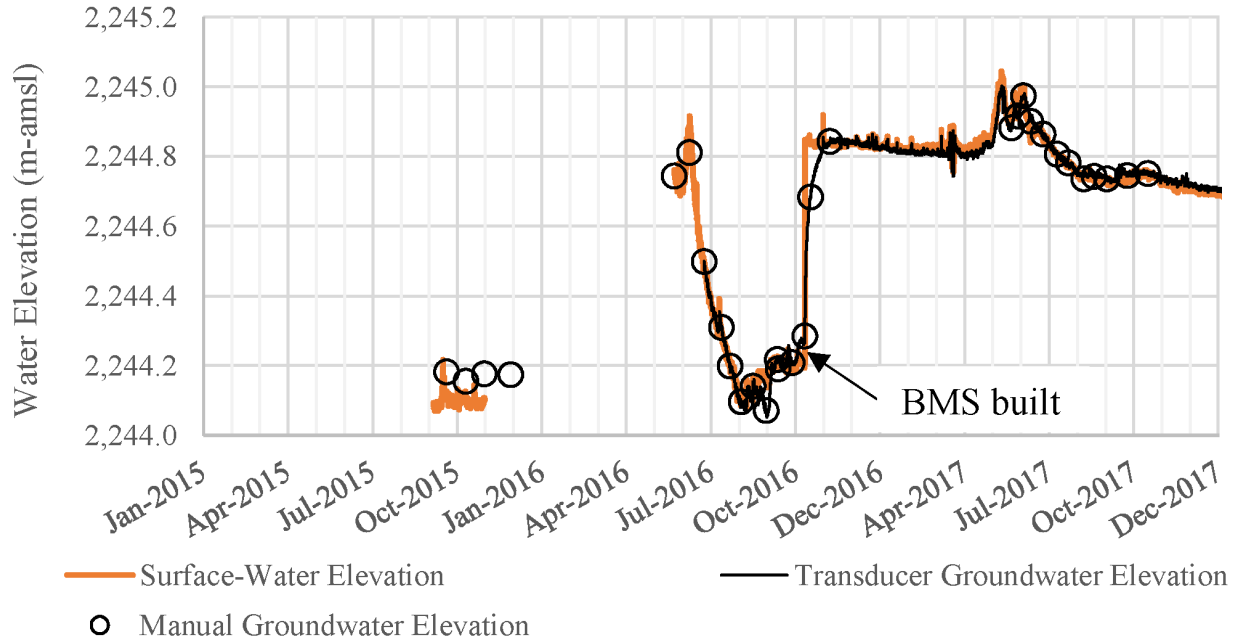
^{*} for testing the effects of ET_{max} ET_{XD} was set to 2 m, and for testing ET_{XD} ET_{max} was set to 600 mm yr^{-1} .



1131

1132 FIGURE S2.4. Changes in Gross Stream Gain caused by implementing the FC scenario with different
 1133 model parameters. Note the different y-scale on the chart for streambed conductance.

1134 S3. Monitoring Example



1135

1136 Figure S3.1. BMR was conducted at Alkali Creek in southwest Montana, USA. A piezometer (A8-
1137 GW1A; GWICID 287986; www.mbm.gwic.mtech.edu) located adjacent to a pond created by a BMS
1138 showed a 0.6 m increase in August groundwater elevation following treatment. A surface-water staff gage
1139 (A8-SW1; GWICID 286976) located in the backwater of the BMS shows a similar rise, with the
1140 groundwater response being somewhat buffered relative to the change in surface-water elevation. Water
1141 levels declined slightly over time as the BMS eroded.

1142

1143 *Literature Cited*

- 1144 Anderson, M.P., Woessner, W.W., Hunt, R.J., 2015. Applied Groundwater Modeling, Applied
1145 Groundwater Modeling. Elsevier. <https://doi.org/10.1016/C2009-0-21563-7>
- 1146 Aquaveo, L., 2013. Groundwater Modeling System (GMS), v. 9.2.
- 1147 Banta, E.R., 2000. MODFLOW-2000, the U.S. Geological Survey Modular Ground-Water Model;
1148 documentation of packages for simulating evapotranspiration with a segmented function (ETS1) and
1149 drains with return flow (DRT1).
- 1150 Barnes, H.H., 1969. Roughness characteristics of natural channels. *J. Hydrol.* 7, 354.
1151 [https://doi.org/10.1016/0022-1694\(69\)90113-9](https://doi.org/10.1016/0022-1694(69)90113-9)
- 1152 Brunner, P., Simmons, C.T., Cook, P.G., Therrien, R., 2010. Modeling surface water-groundwater
1153 interaction with MODFLOW: Some considerations. *Ground Water* 48, 174–180.
1154 <https://doi.org/10.1111/j.1745-6584.2009.00644.x>
- 1155 Fetter, C.W., 1994. Applied Hydrogeology, 3rd ed. Prentice Hall, Upper Saddle River, NJ.
- 1156 Freeze, R.A., Cherry, J.A., 1979. Groundwater, 1st ed. Prentice-Hall Inc, Englewood Cliffs, NJ.
- 1157 Harbaugh, A.W., Banta, E.R., Hill, M.C., McDonald, M.G., Groat, C.G., 2000. MODFLOW-2000, The
1158 U. S. Geological Survey modular ground-water model user guide to modularization concepts and the
1159 ground-water flow process. USGS Open-File Rep. 00–92, 121.
- 1160 Heath, R.C., 1983. Basic Ground-Water hydrology. USGS Water-Supply Pap. 2220, 86.
- 1161 McDonald, M.G., Harbaugh, A.W., 1988. A modular three-dimensional finite-difference groundwater
1162 flow model, Techniques of Water-Resources Investigations Report, 06-A1. Methods Determ. ...
1163 588. [https://doi.org/10.1016/0022-1694\(70\)90079-X](https://doi.org/10.1016/0022-1694(70)90079-X)
- 1164 Niswonger, R.G., Prudic, D.E., 2005. Documentation of the Streamflow-Routing (SFR2) Package to
1165 include unsaturated flow beneath streams - A modification to SFR1, in: US Geological Survey:
1166 Book 6: Modeling Techniques. p. 47. <https://doi.org/Techniques and Methods 6-A13 version 1.10>
- 1167 Prudic, D.E., 1989. Documentation of a computer program to simulate stream-aquifer relations using a
1168 modular, finite-difference, ground-water flow model. USGS Open-File Rep. 88–729, 113.
1169 <https://doi.org/10.3133/ofr88729>
- 1170 Shah, N., Nachabe, M., Ross, M., 2007. Extinction depth and evapotranspiration from ground water under
1171 selected land covers. *Ground Water* 45, 329–338. <https://doi.org/10.1111/j.1745-6584.2007.00302.x>
- 1172 Winter, T.C., Harvey, J.W., Franke, O.L., Alley, W.M., 1998. Groundwater and surface water a single
1173 resource. USGS Circ. 1139, 87. <https://doi.org/10.3133/CIR1139>
- 1174